

# Novel electromagnetic structures for high frequency acceleration (Part 4-6)

Rosa Letizia

Lancaster University/ Cockcroft Institute

[r.letizia@lancaster.ac.uk](mailto:r.letizia@lancaster.ac.uk)

Cockcroft Institute, Spring term, 13/03/17

# Lectures outline

## Lecture 4 – Introduction to Metamaterials

- Novel electromagnetic properties
- Dispersion engineering
- Metamaterials loaded waveguides
- Potential application in accelerators

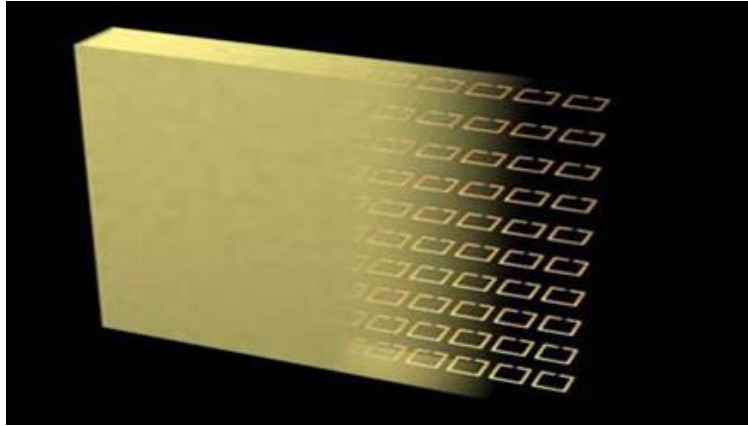
## Lecture 5 – Introduction to Plasmonic waveguiding

- Surface plasmon polariton
- Dispersion
- Plasmonic waveguide
- Accelerators applications

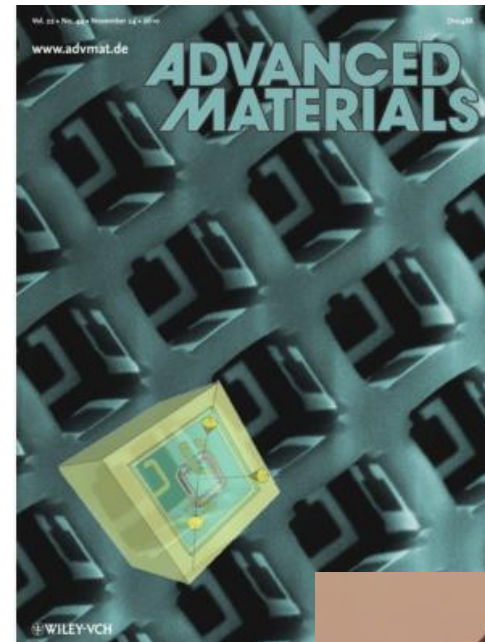
## Lecture 6 – Introduction to Finite Difference Time Domain

- Time domain computational modelling
- Finite Difference Time Domain
- Examples

# “Beyond” (Meta) materials

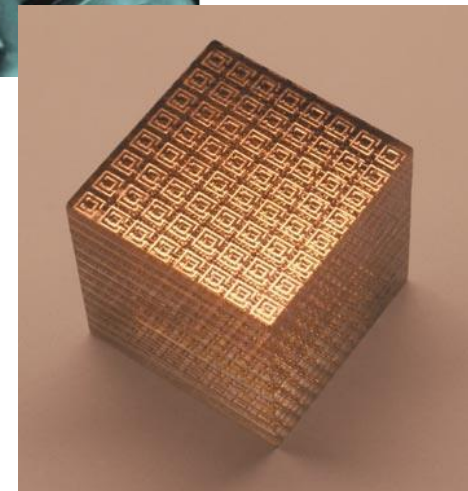


<http://metamaterials.duke.edu/research/metamaterials/retrieval>



The term “Metamaterial” is first coined by Rodger Walser as (2001/2):

*‘Macroscopic composites having man-made, three dimensional, periodic cellular architecture designed to produce an optimised combination, not available in nature, of two or more responses to specific excitation.’*

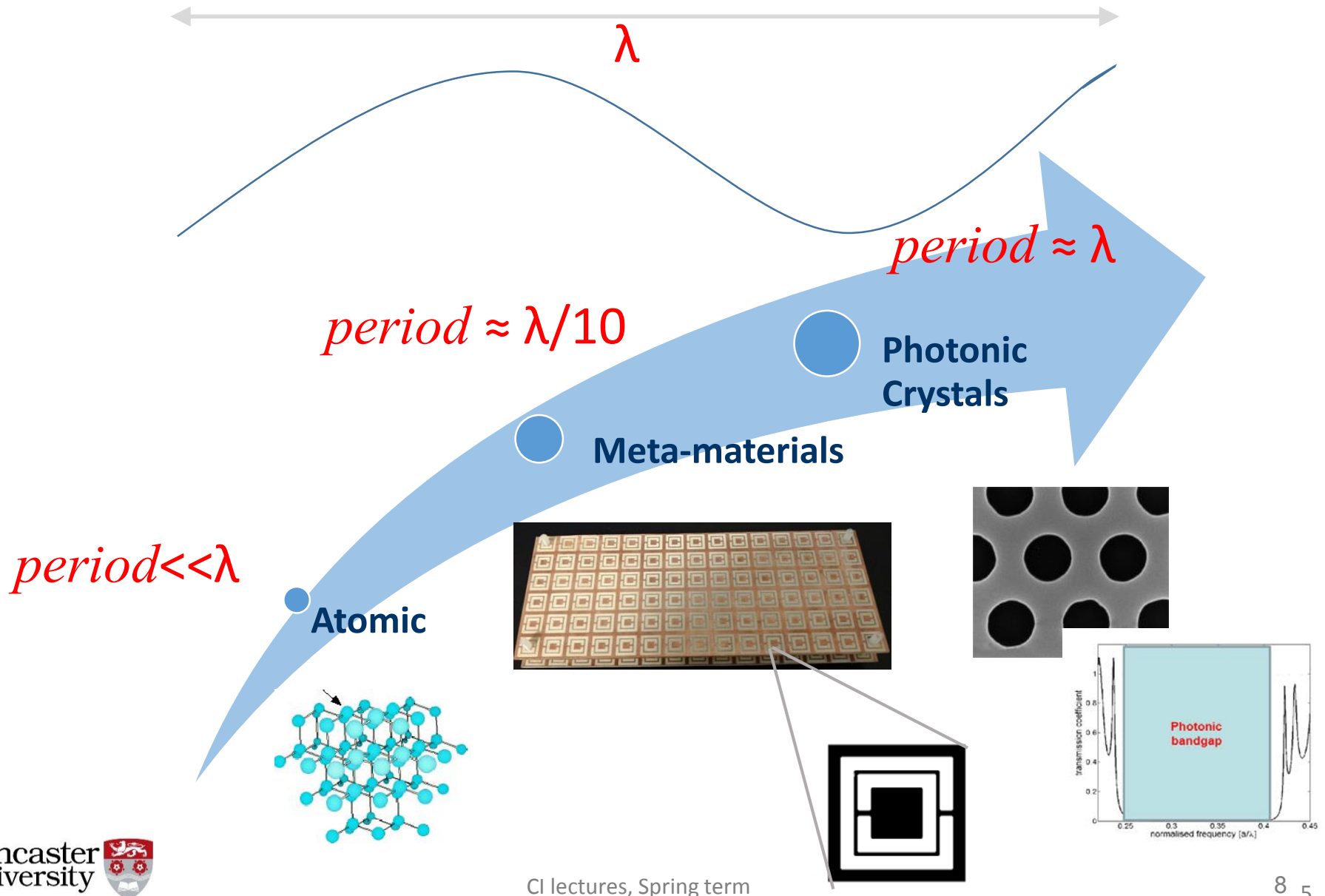


# Meta-materials



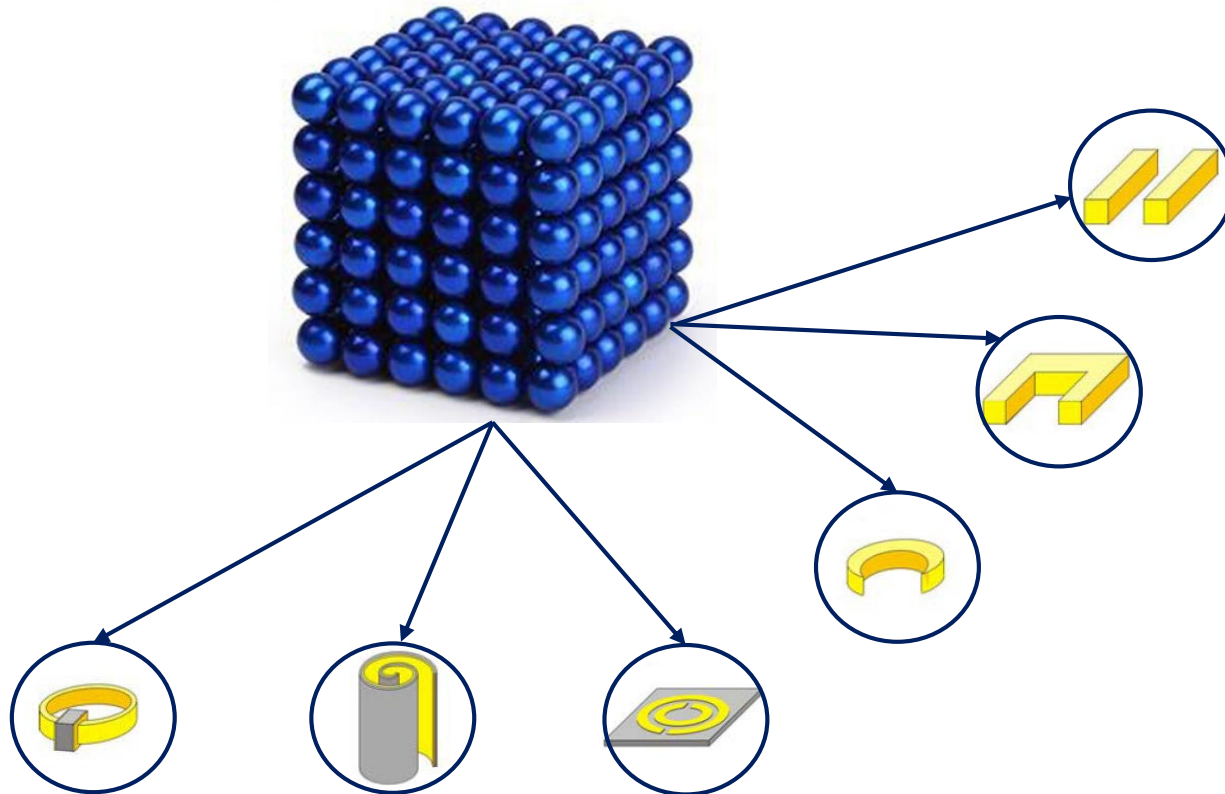
**Lycurgus Cup – British Museum**

# Dispersion engineering



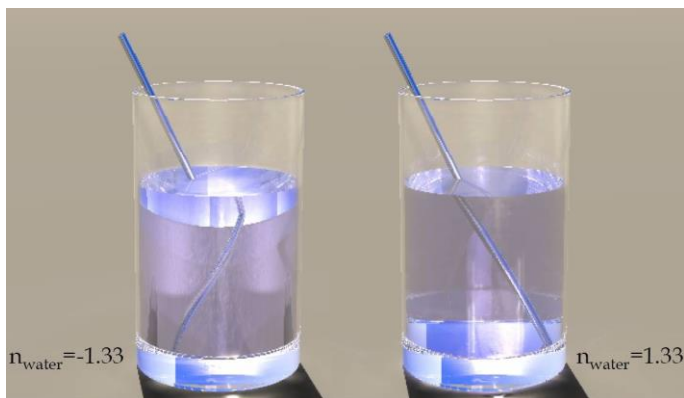
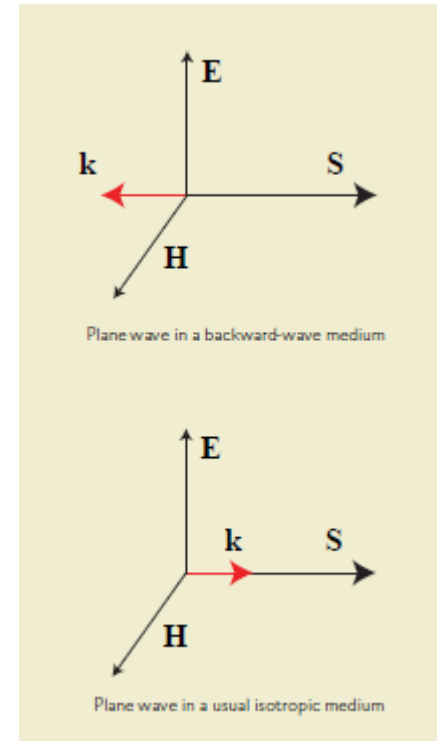
# Artificial electromagnetic materials

- Control the flow of EM wave in unprecedented way
- The design relies on inclusions and the new properties emerge due the specific interactions with EM fields
- These designs can be scaled down and the MTM really behaves as an effectively continuous medium



# Negative Refractive index

- Negative refractive index materials do not exist in nature. These type of materials were first theoretically introduced by **Veselago (1968)** but only in 90's **Pendry/Smith** showed how to physically realise them.
- Backward wave media are materials in which the energy velocity direction is opposite to the phase velocity direction. In particular this takes place in isotropic materials with negative permittivity and permeability (**double negative materials, DNM or negative index materials, NIM**).

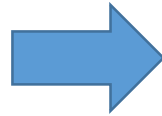


- Reverse Snell's law of refraction
- Reverse Cherenkov effect
- Reverse Doppler effect

# Negative Refraction

$$\sqrt{\epsilon_r} = j\sqrt{|\epsilon_r|}$$

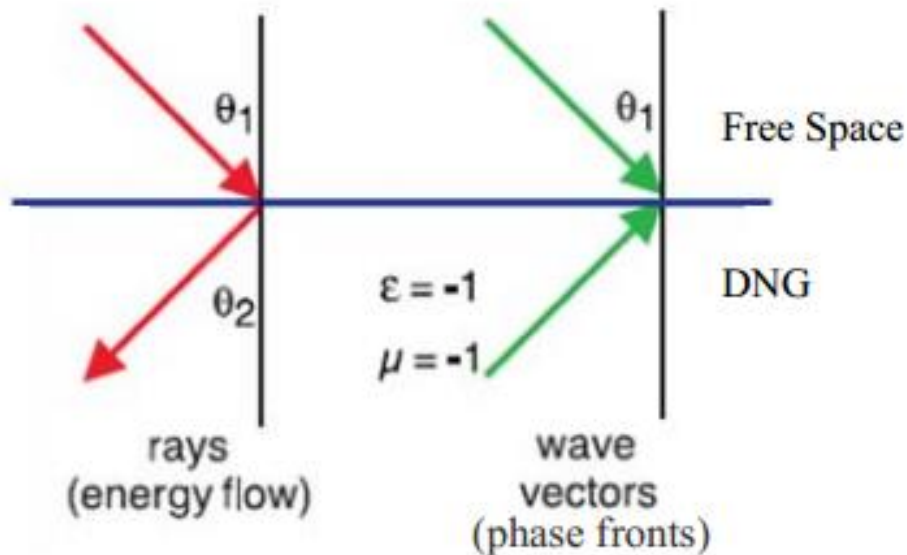
$$\sqrt{\mu_r} = j\sqrt{|\mu_r|}$$



$$n = \sqrt{\epsilon_r \mu_r} = -\sqrt{|\epsilon_r| |\mu_r|}$$

MTMs obey Snell's law:

$$n_1 \sin \theta_1 = n_2 \sin \theta_2$$

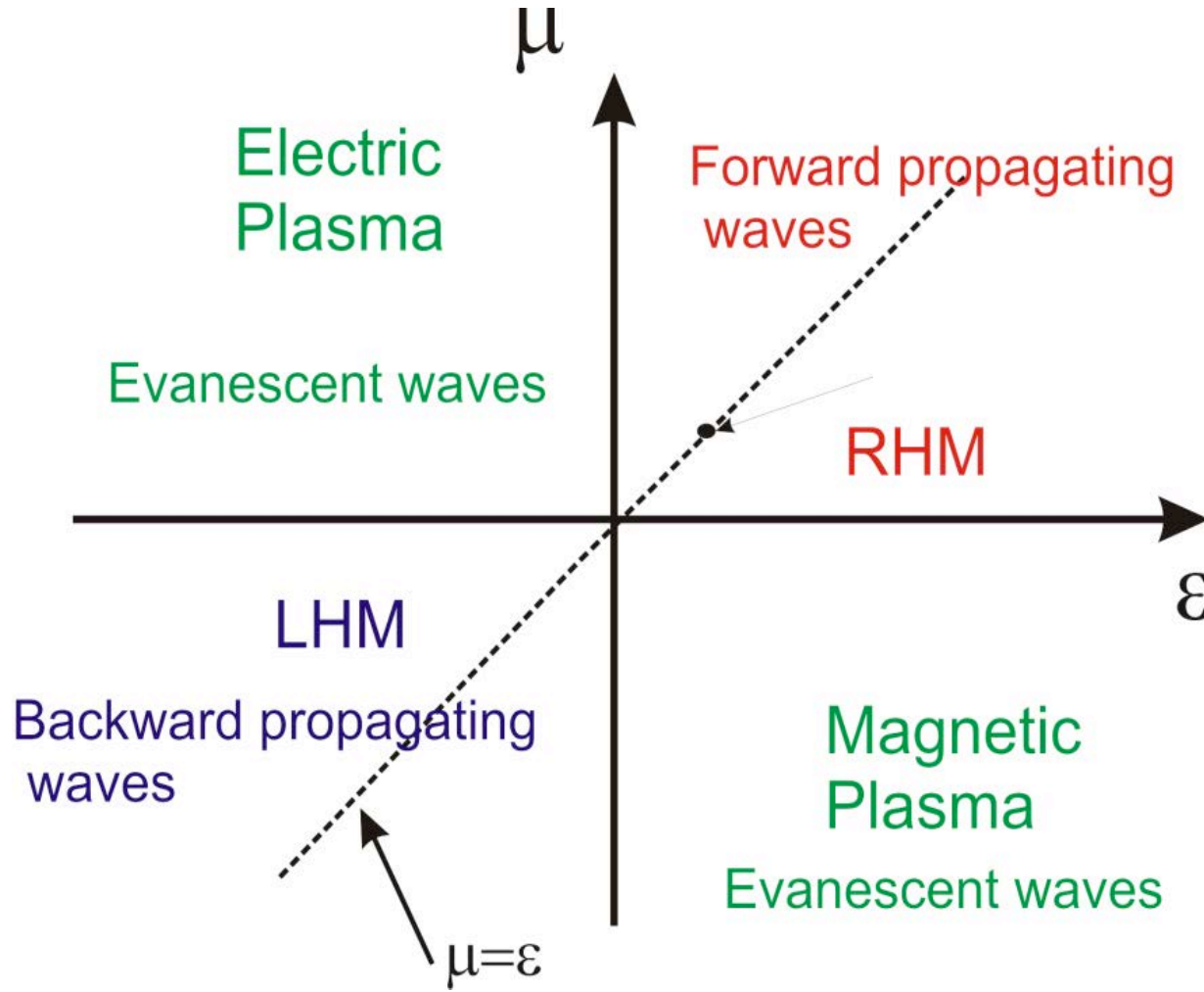


$$\theta_2 < 0$$

Negative refraction takes place at the interface between “normal” media and a double negative material

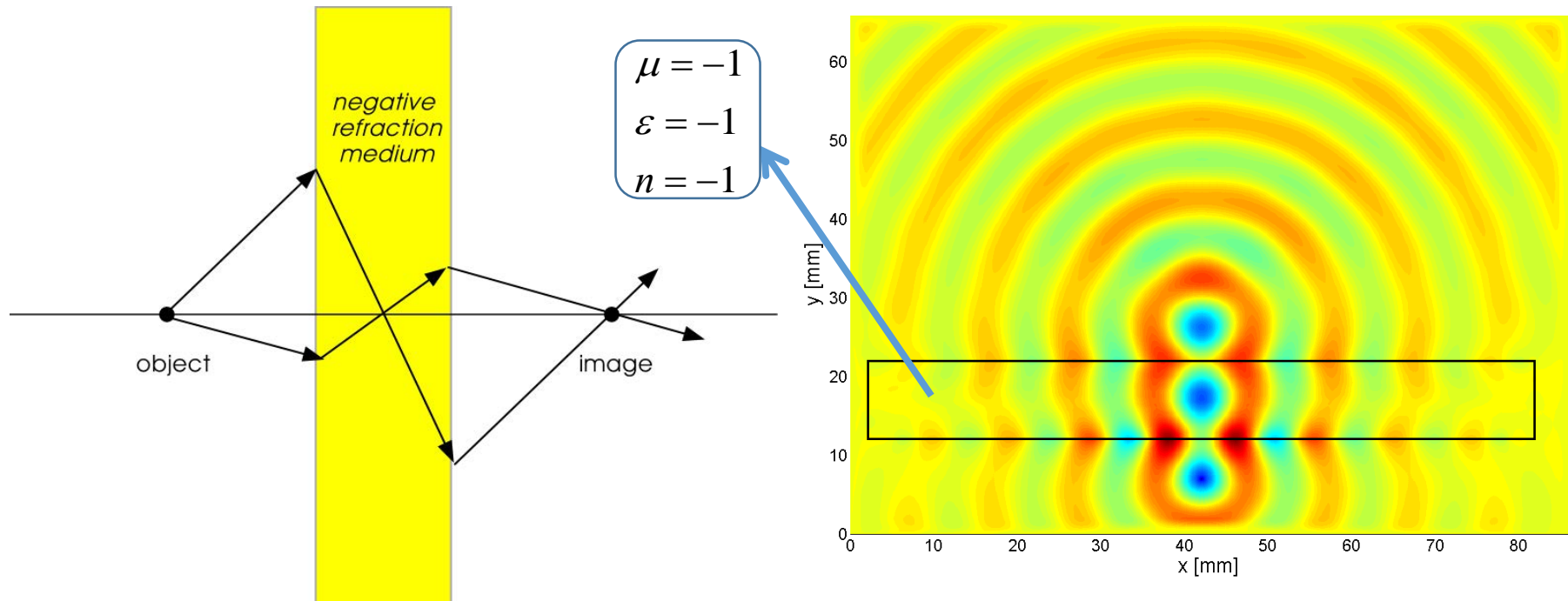


# Designing the EM response

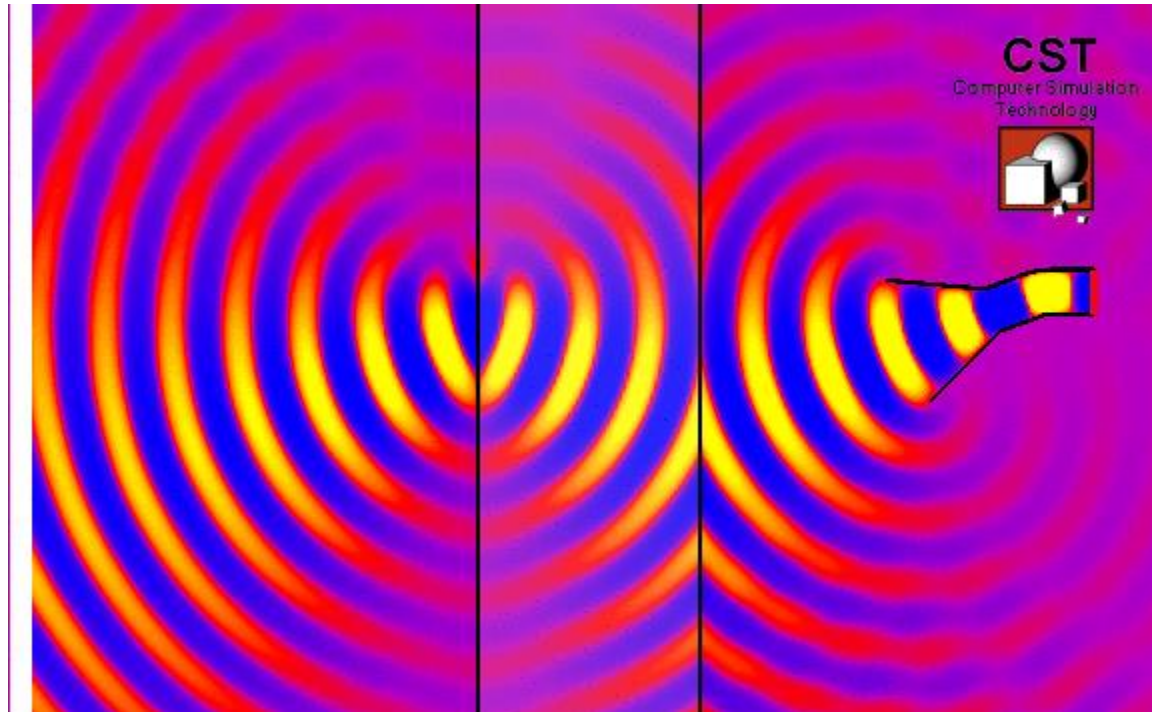


# Focusing - Perfect lens

- Negative refraction can be used to focus light. A flat slab of material will produce two focal points, one inside the slab and the other one outside.
- UNUSUAL focussing properties.
  - no reflection from surfaces
  - aberration-free focus
  - free from wavelength restriction on resolution



# Negative refraction



# Negative permittivity

- Bulk metal – Drude response

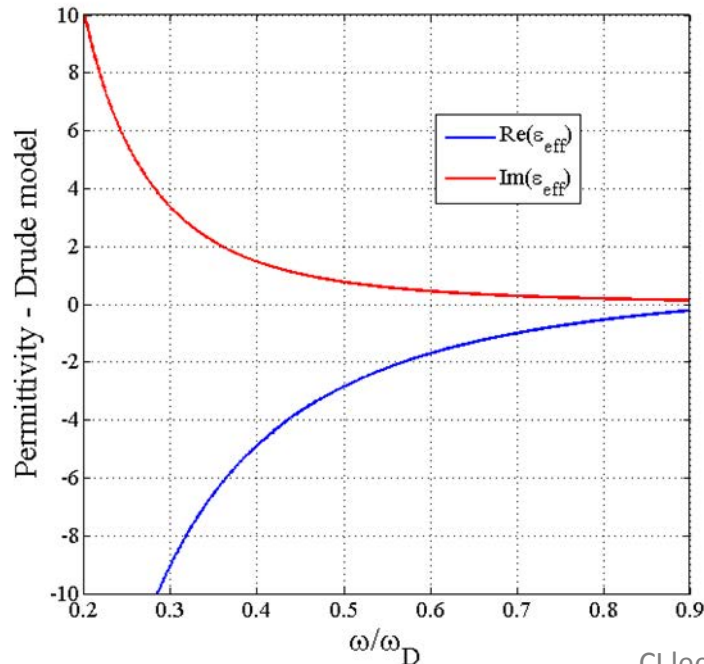
$$\epsilon(\omega) = 1 - \frac{\omega_p^2}{\omega(\omega + i\gamma)}$$

- PLASMA FREQUENCY

$$\omega_p^2 = \frac{Ne^2}{\epsilon_0 m}$$

(frequency with which the collection of free electrons (plasma) oscillates in the presence of an external driving field)

- When  $\gamma = 0$  and  $\omega < \omega_p \rightarrow \epsilon < 0$



## Limitations:

- $\omega_p$  is typically in the ultraviolet range
- For  $\omega < \omega_p$  the response is dominated by the imaginary component  $\rightarrow$  high losses

# Artificial negative permittivity – Wire medium

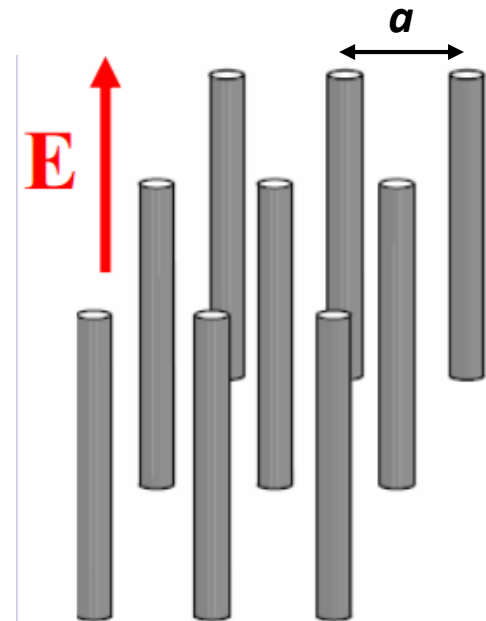
- Bulk metal – Drude response  $\epsilon(\omega) = 1 - \frac{\omega_p^2}{\omega(\omega + i\gamma)}$
- Artificial negative permittivity – “Wire medium” (Pendry et al. 1998)
  - The plasma frequency depends critically on density and mass of the collective electronic motion

$E = E_0 e^{-i(\omega t - kz)}$ , The whole structure appears as an **effective medium** whose electrons (in the wires) move in the +z direction.

$\lambda \gg a$

$N_{eff} = N \frac{\pi r^2}{a^2} \ll N$  (electron density within each wire)

$m_{eff} = 0.5 \mu_0 N e^2 r^2 \ln(a/r) \gg m$  (free electron mass)



$$\omega_p^2 = \frac{N_{eff} e^2}{\epsilon_0 m_{eff}} = \frac{2\pi c^2}{a^2 \ln(a/r)} \rightarrow f_p = \omega_p / 2\pi \ll \text{metal plasma freq.}$$

## Negative permeability – Split ring resonator

- Negative permeability does not normally occur in natural materials.
- Pendry et al. suggested that an array of ring resonators (SRRs) could respond to the magnetic component of the light.

$$H = H_0 e^{i(\omega t - kx)}$$

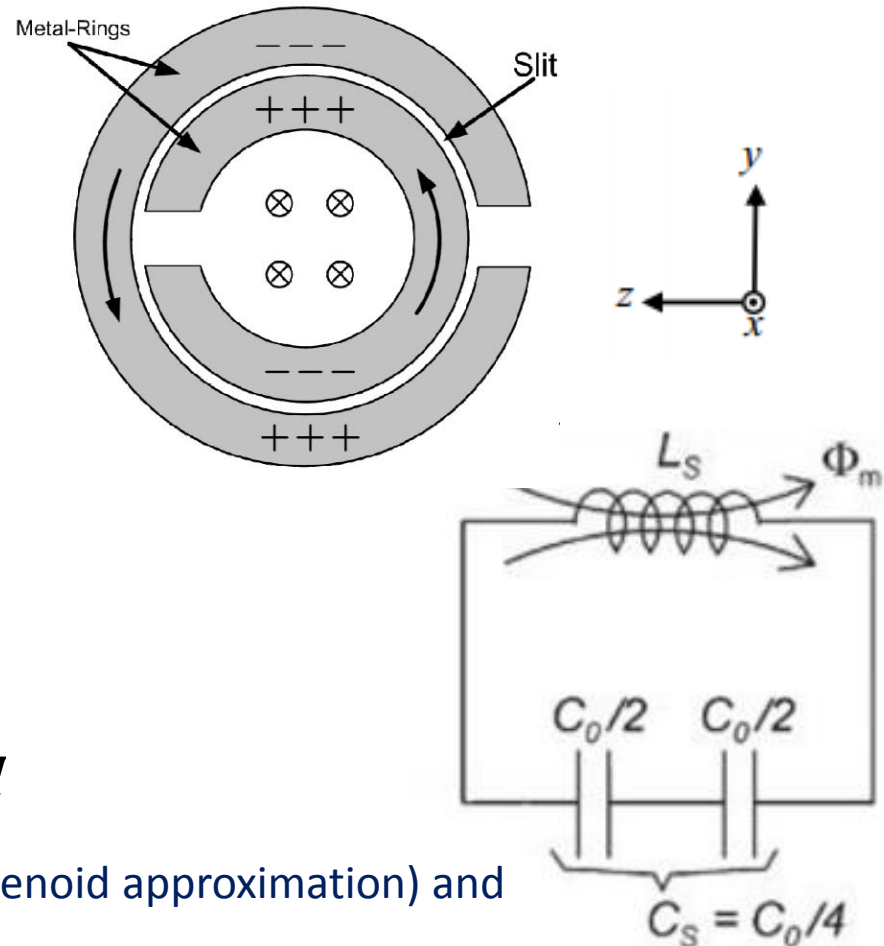
$$U = i\omega\mu_0\pi r^2 H_0$$

$$\Phi = \mu_0\pi r^2 I/l$$

$$L = \frac{\Phi}{I} = \frac{\mu_0\pi r^2}{l}$$

$$M = \frac{\pi r^2}{a^2} L = FL$$

$$U = [R + i/(\omega c) - i\omega L + i\omega M] I$$



where  $l$  = distance in x between SRRs (solenoid approximation) and  $R$  is the ohmic resistance of each ring.

# Negative permeability – Split ring resonator

- Negative permeability does not normally occur in natural materials.

$$M_d = I \frac{\pi r^2}{a^2 l}, \quad I = - \frac{H_0 l}{(1-F) - 1/(\omega^2 LC) + i R/(\omega L)}$$

$$\mu_r = \frac{B/\mu_0}{B/\mu_0 - M_d} = 1 - \frac{F}{1 - 1/(\omega^2 LC) + i R/(\omega L)}$$

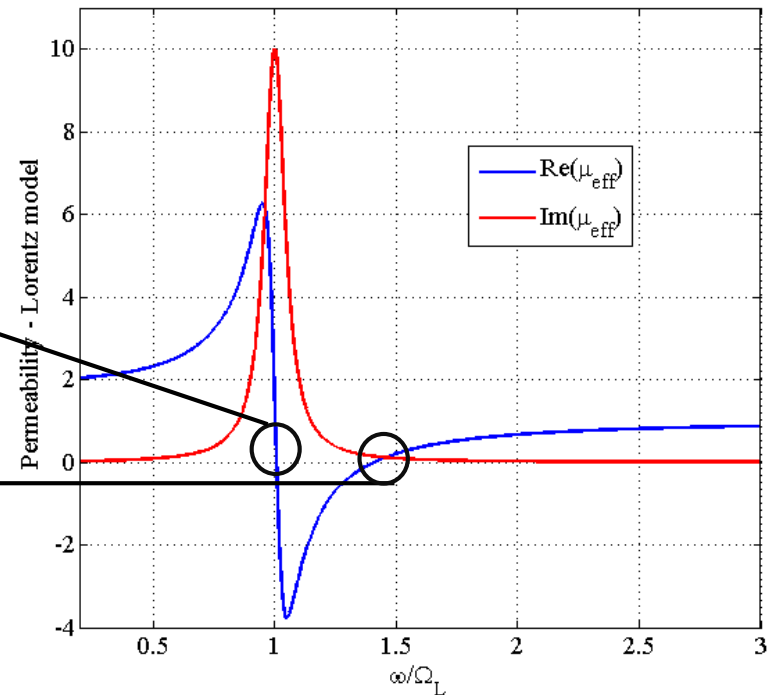
(in the direction x)

$$\omega_{m0} = \frac{1}{\sqrt{LC}}$$

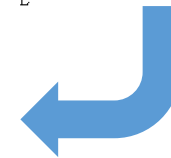
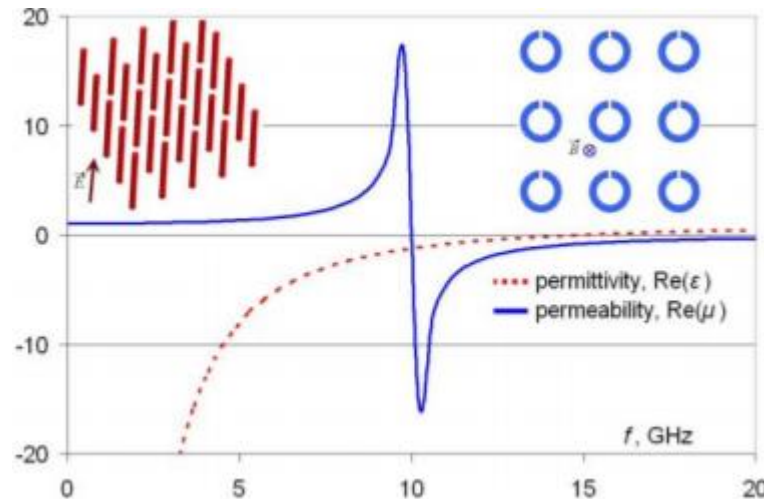
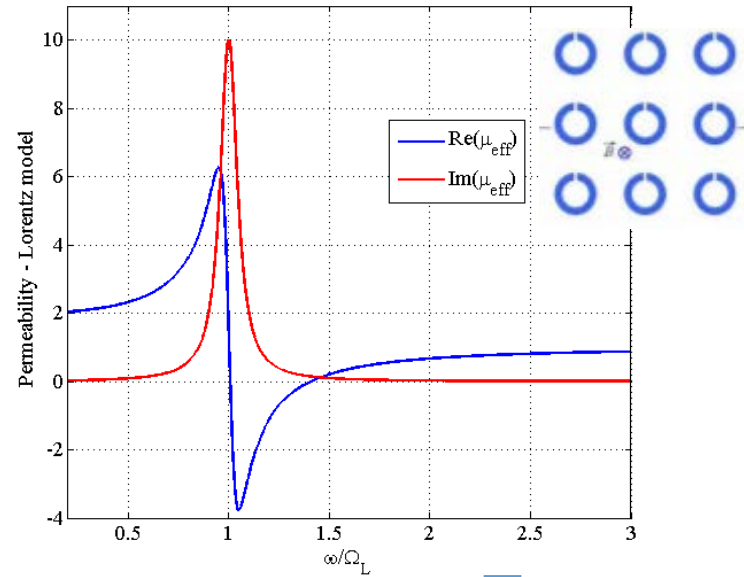
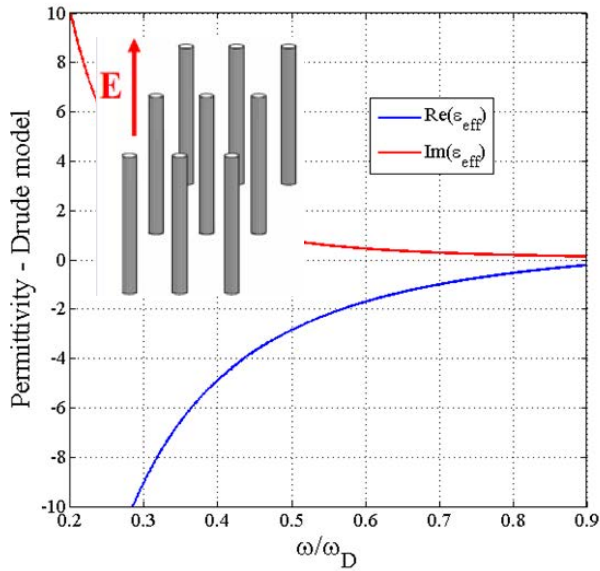
Resonance frequency  
of the Lorentzian  
variation of the  
medium's effective  
permeability

$$\omega_{mp} = \frac{1}{\sqrt{LC(1-F)}}$$

Plasma frequency



# Left-handed material



[Antipov et al, *Proc. IPAC* (2007)]

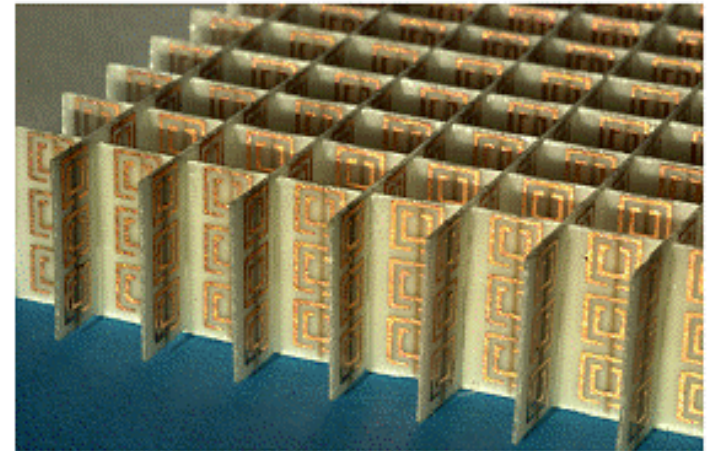
[Smith et al, *Phys Rev Letts*, 84, (2000)]



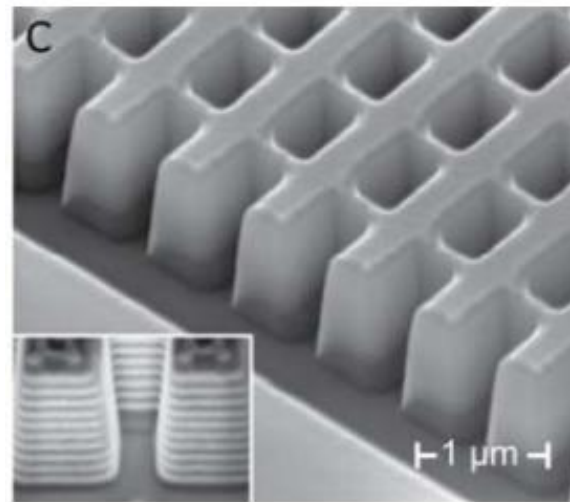
# Left-handed material



microwave range (Smith et al., 2000)



microwave range (Smith et al., 2004)



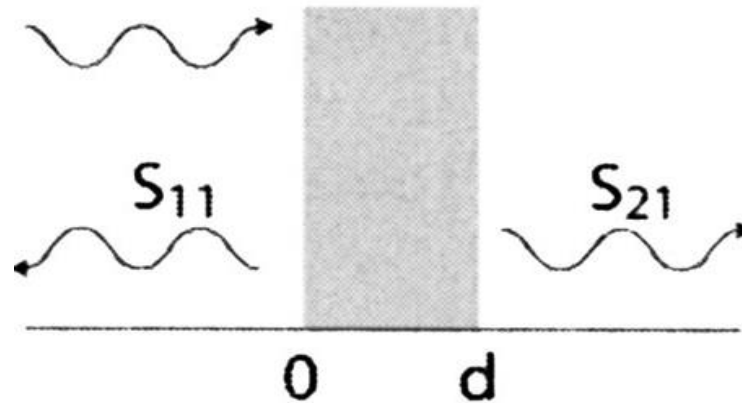
NIR range (X. Zhang et al., 2008)

## Retrieving the effective parameters

S-parameters are defined in terms of **reflection coefficient R** and **transmission coefficient T**:

$$S_{11} = R$$

$$S_{21} = T e^{jk_0 d}$$



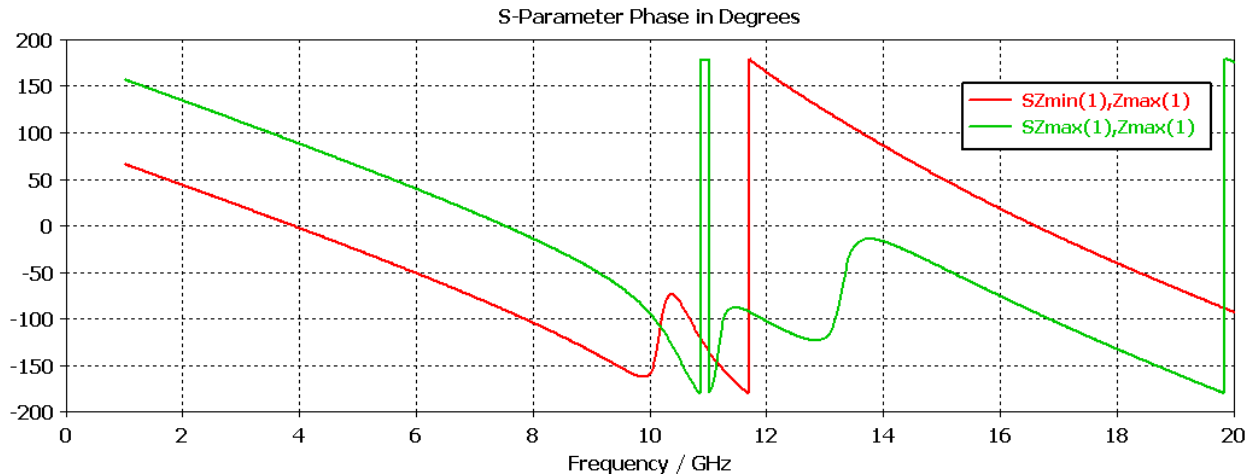
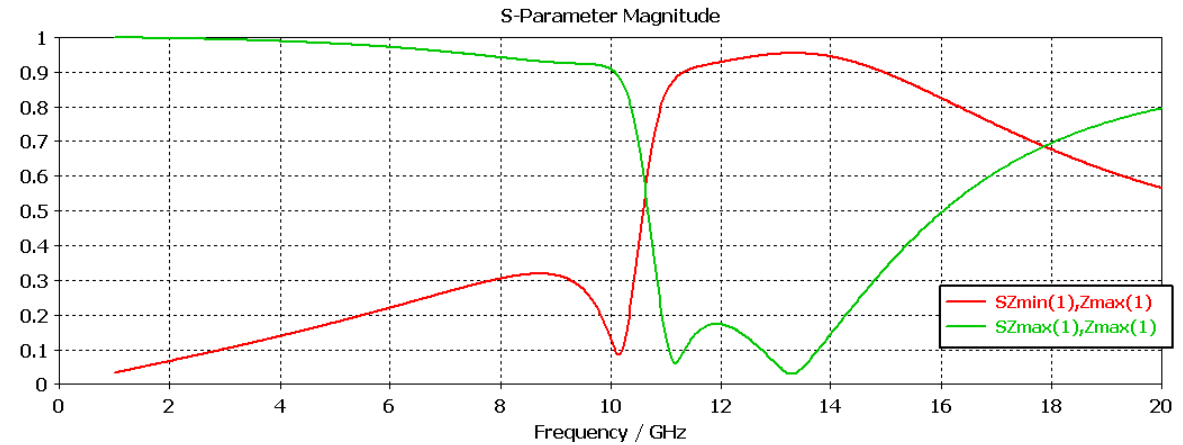
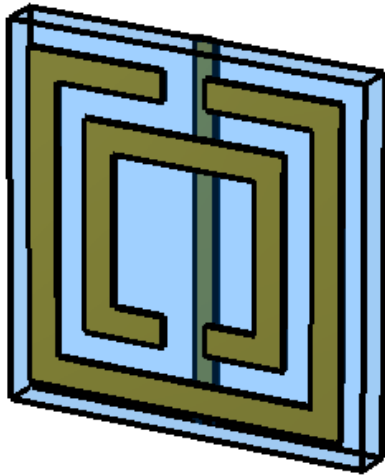
$$Z = \pm \sqrt{\frac{(1 + S_{11})^2 - S_{21}^2}{(1 - S_{11})^2 - S_{21}^2}}$$

$$n = \frac{1}{k_0 d} \left\{ \left[ \text{Im}[\ln(e^{jn k_0 d})] + 2m\pi \right] - j \left[ \text{Re}[\ln(e^{jn k_0 d})] \right] \right\}$$

$$e^{jn k_0 d} = \frac{S_{21}}{1 - S_{11} \frac{Z - 1}{Z + 1}}$$

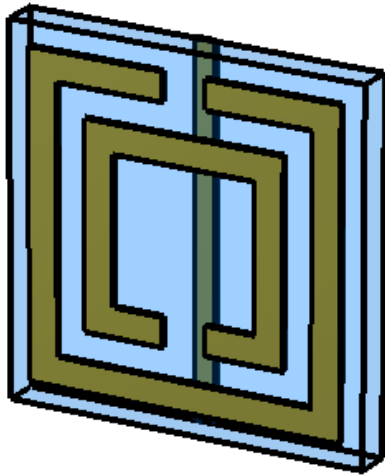
# A numerical example

Negative index MTM (unit cell): SRR for magnetic resonance and wire for electric resonance (copper on FR4 substrate)

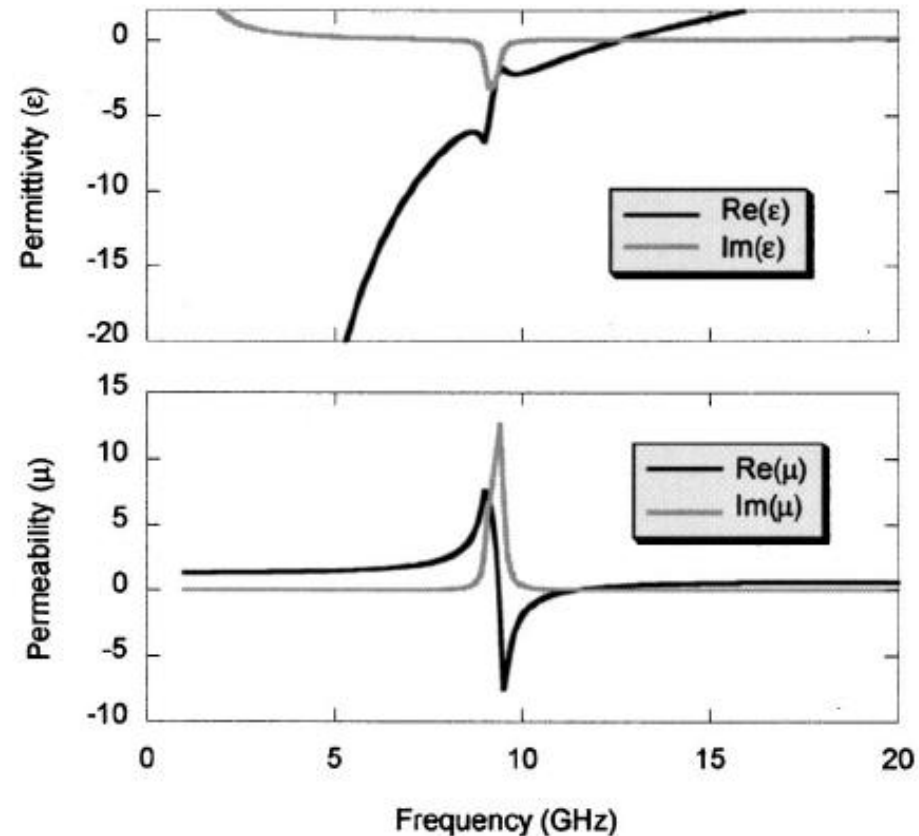


# A numerical example

**Negative index MTM (unit cell):** SRR for magnetic resonance and wire for electric resonance (copper on FR4 substrate)

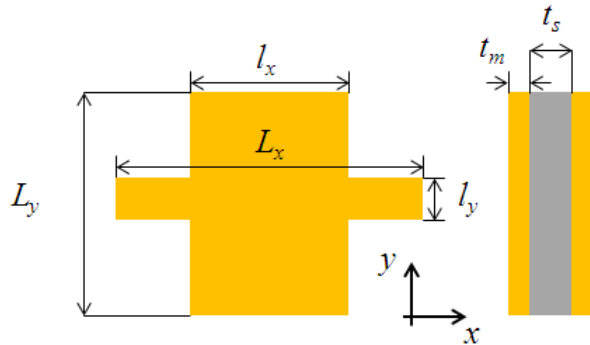


**Calculated permittivity and permeability from S-parameters:**

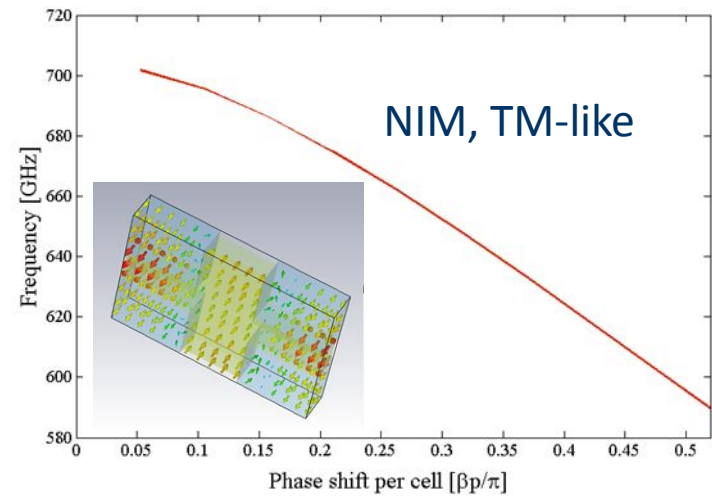
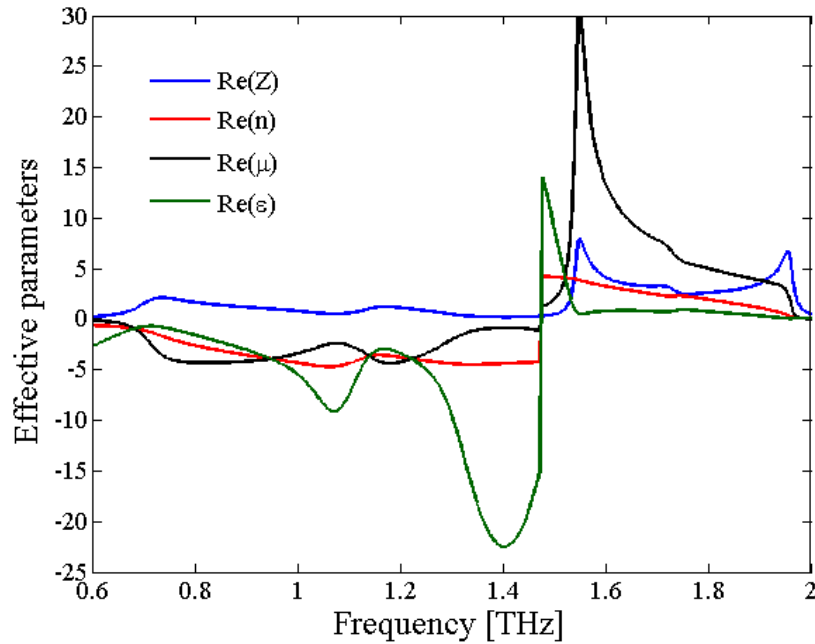
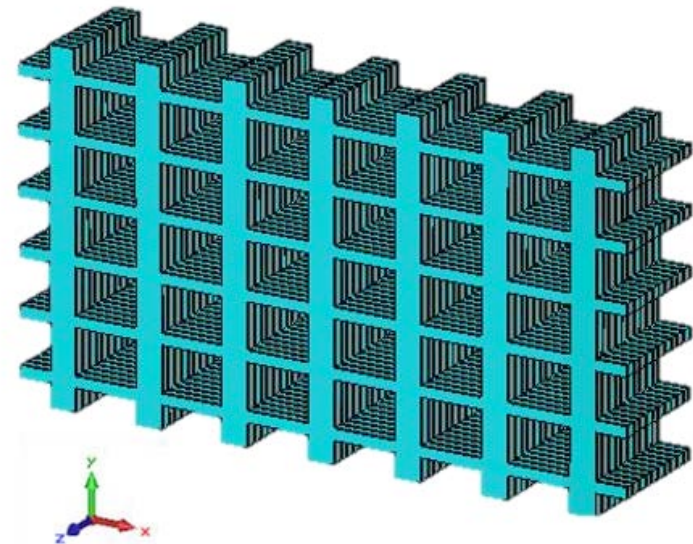


[Smith, Physical Review E, 71, 036617, (2005)]

# Fishnet metamaterial

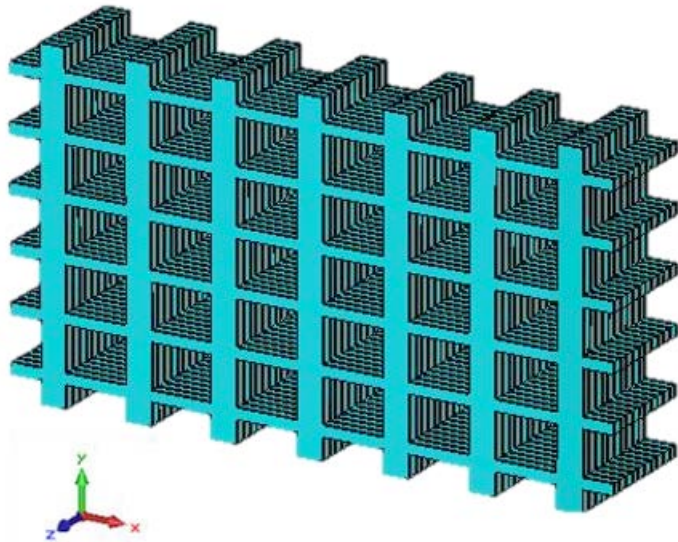


Param.	$L_x$	$L_y$	$l_x$	$l_y$	$t_m$	$t_s$
$\mu\text{m}$	150	97	68	19	4.9	14

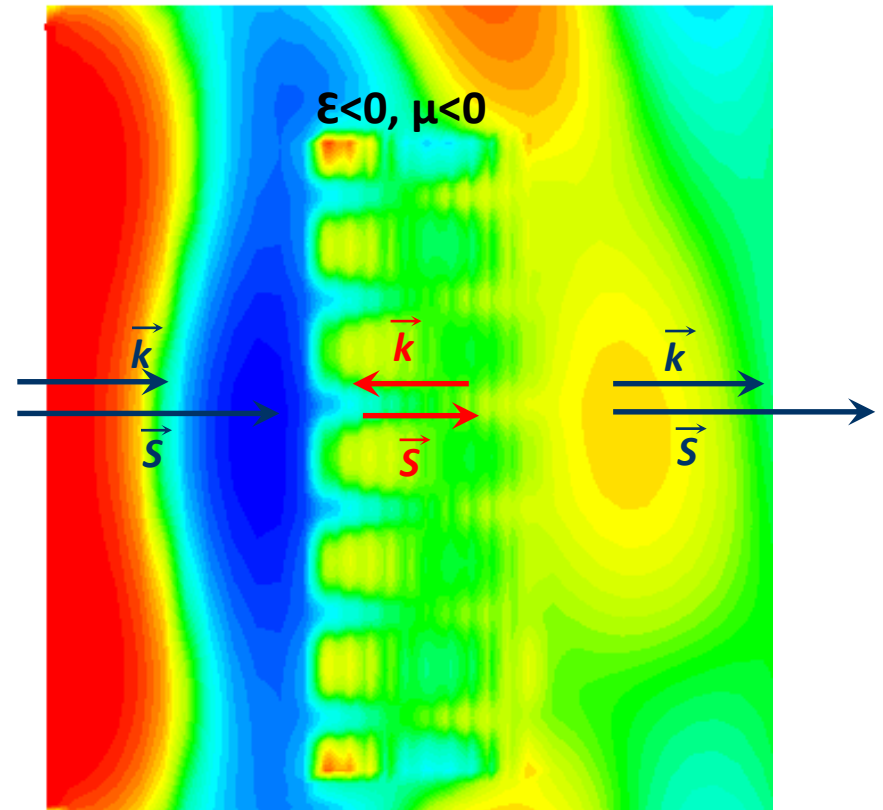


[R. Letizia, *Proc. of UCMMT*, IEEE, (2013)]

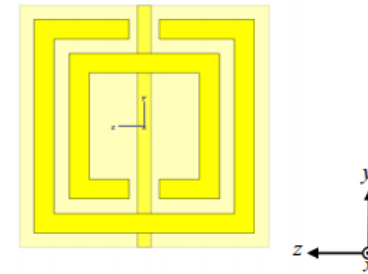
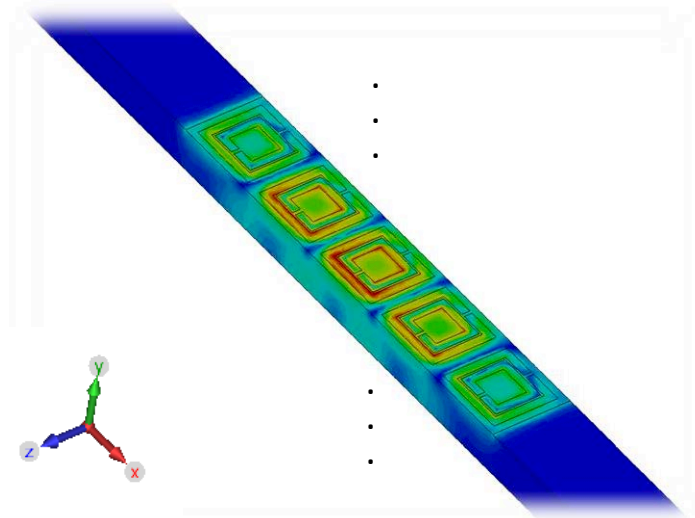
# Fishnet metamaterial



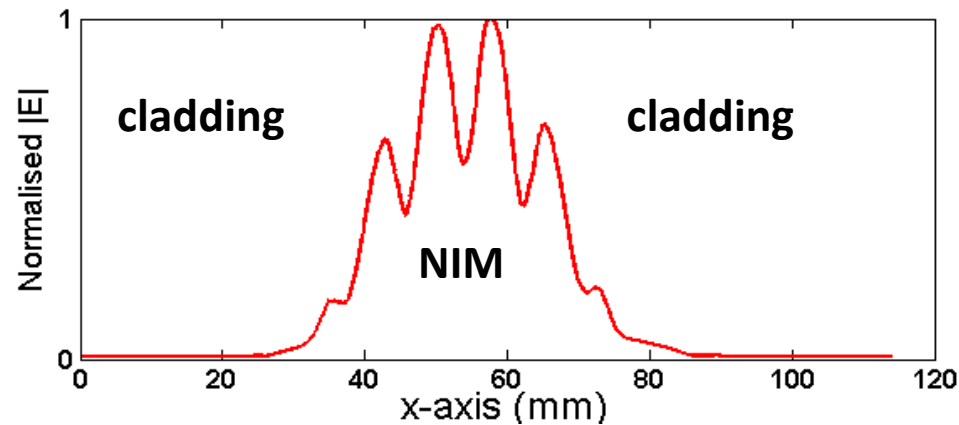
10 periods of fishnet single layer



# Metamaterial waveguides



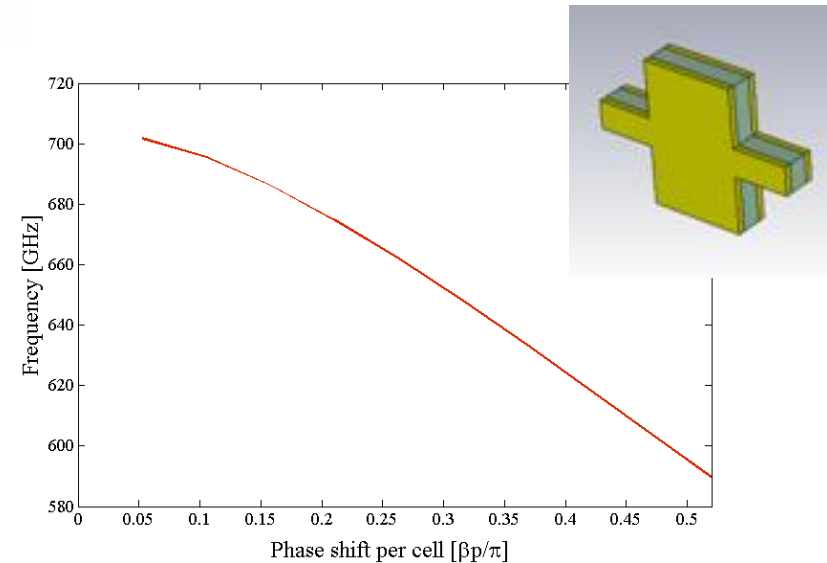
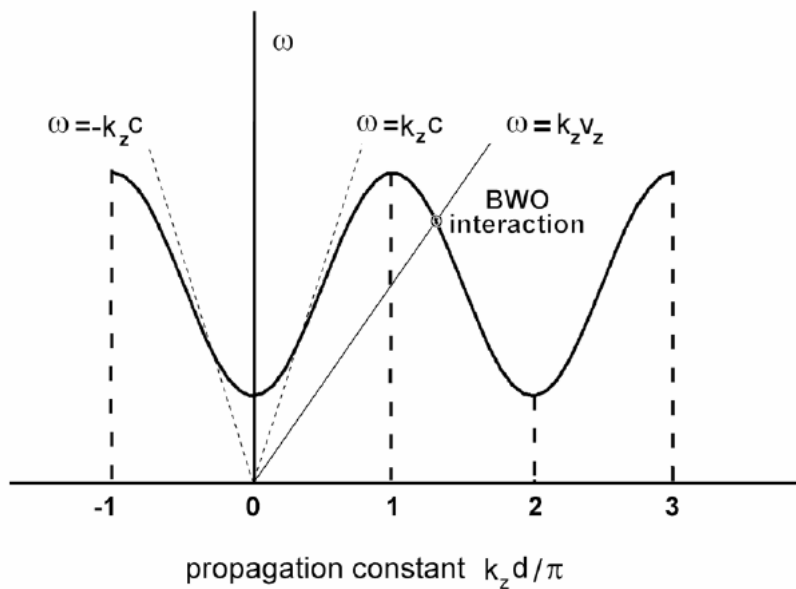
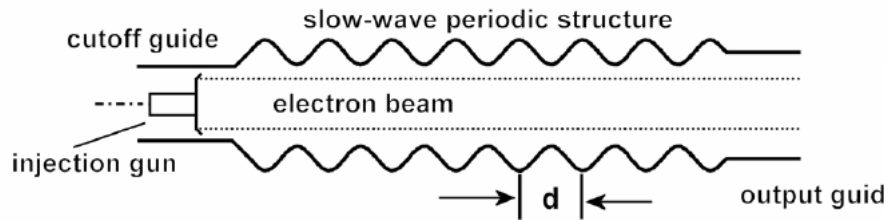
Split Ring Resonators  $\rightarrow \mu < 0$   
Metal wire  $\rightarrow \epsilon < 0$



- Below cut-off propagation and lateral mode confinement without side walls

# Interactions with particle beam

- No need for band-folding given by longitudinal periodicity: fundamental spatial harmonic interacts with sub-relativistic electron beam

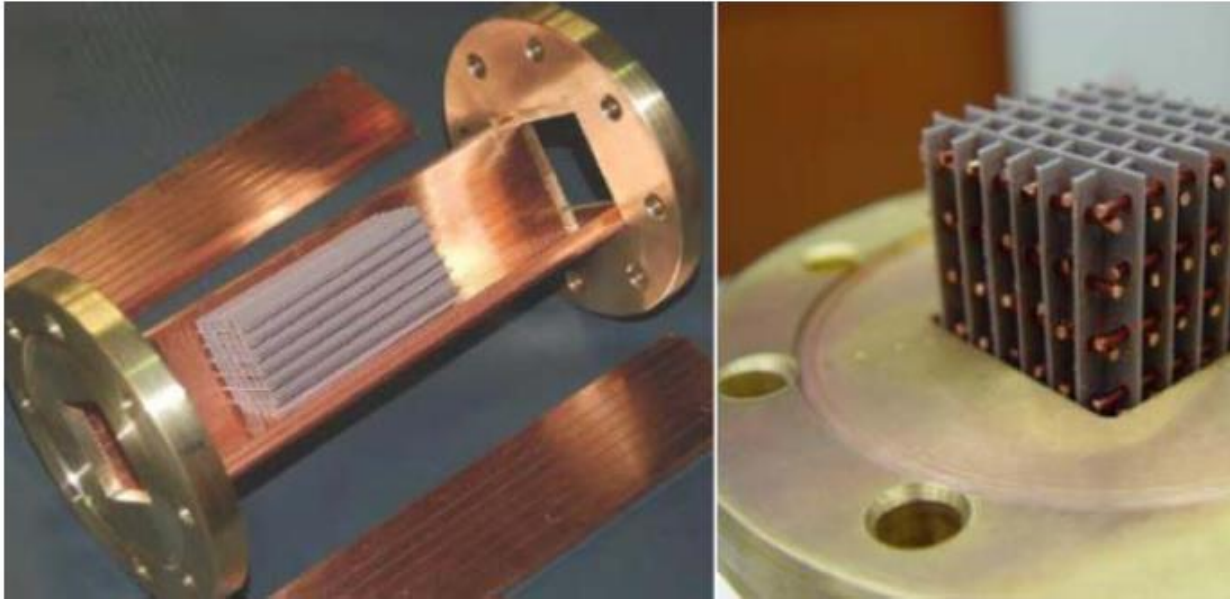


- Possibility of isotropic negative index in bulk metamaterials
- Reverse Cherenkov radiation



# MTM-loaded waveguides

2008, Antipov – first test of electron beam through a NIM medium



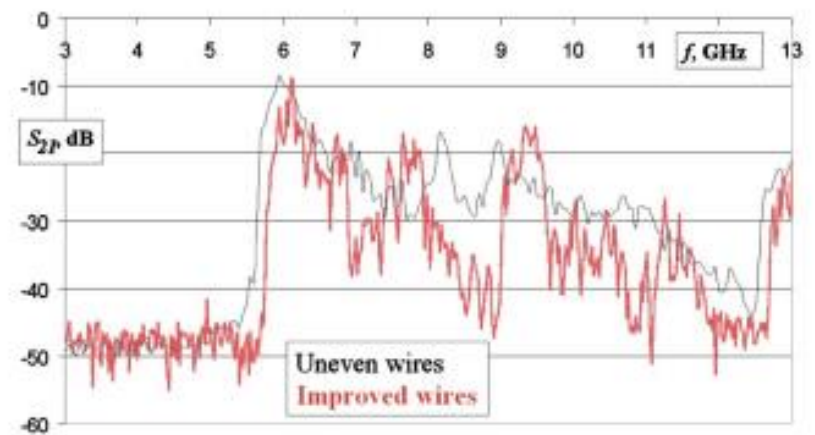
- Metamaterials can be used to generate wakefield (Cherenkov radiation) in accelerating structures (artificial dielectric).
- Slow backwards waves are produced for NIM loaded waveguide.

[Antipov, J. Appl. Phys. **104**, 014901 (2008)]

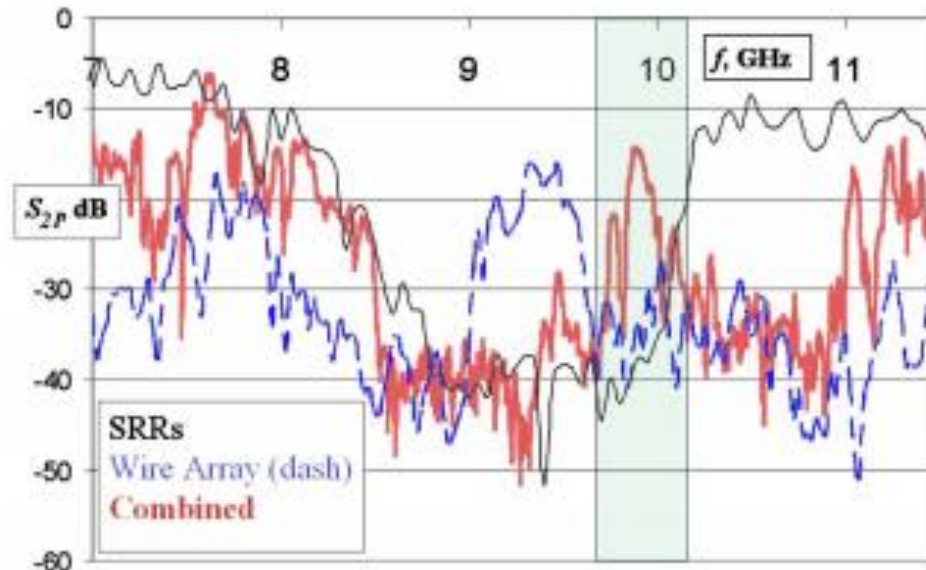
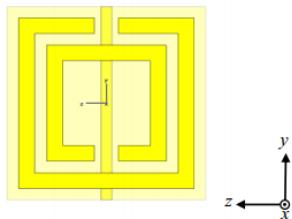
# MTM-loaded waveguides



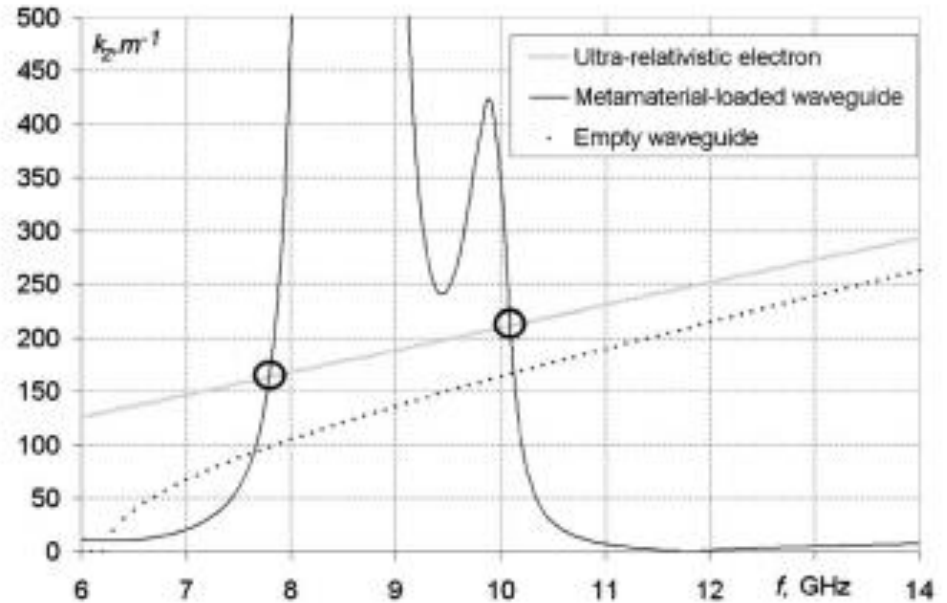
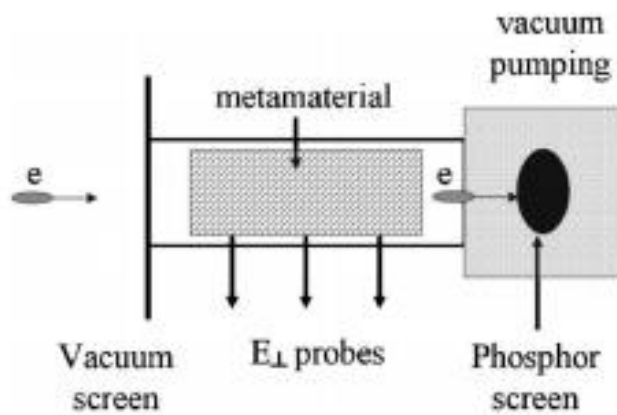
Transmission through only SRRs array



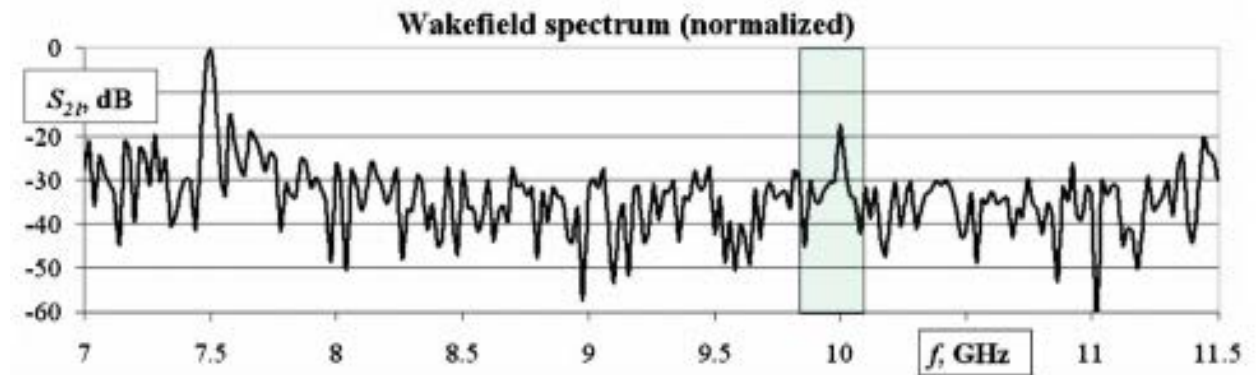
Transmission through only wires array



# MTM-loaded waveguides

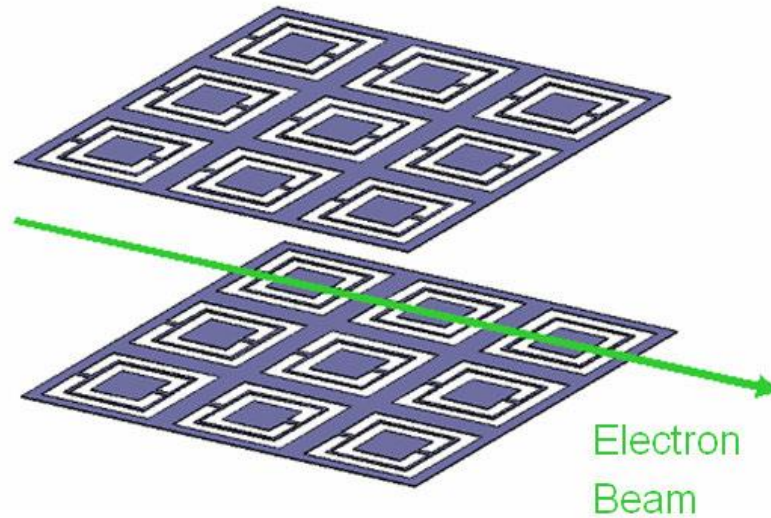


BEAM = 0.25 nC, 3 mm  
(10 ps)  
(longitudinal size)

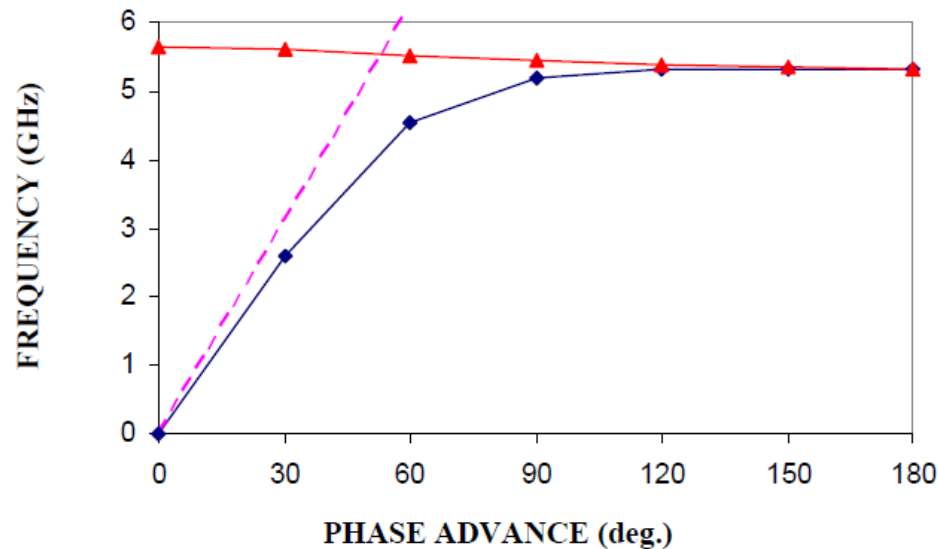


[Antipov, J. Appl. Phys. **104**, 014901 (2008)]

# MTM-loaded waveguides

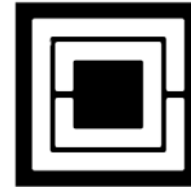
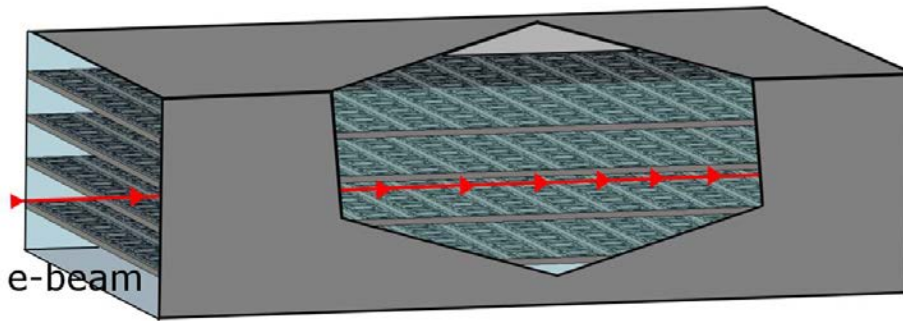


**2009** – An all-metallic proposal:  
Left-handed material based on CSRR  
sheets (spacing = 26 mm)



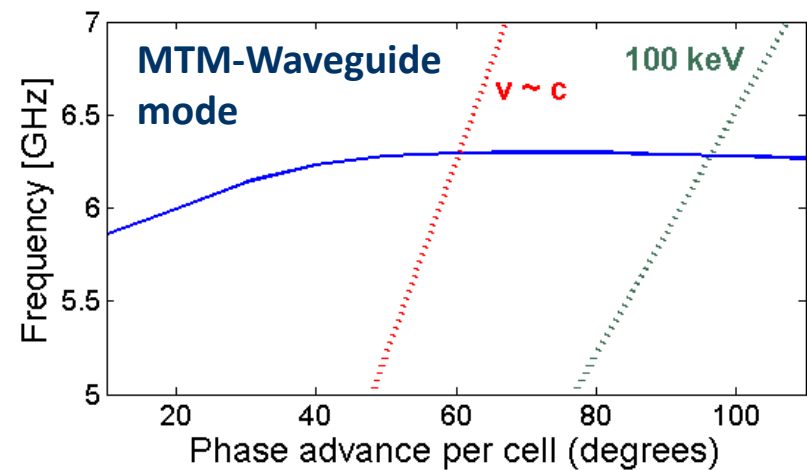
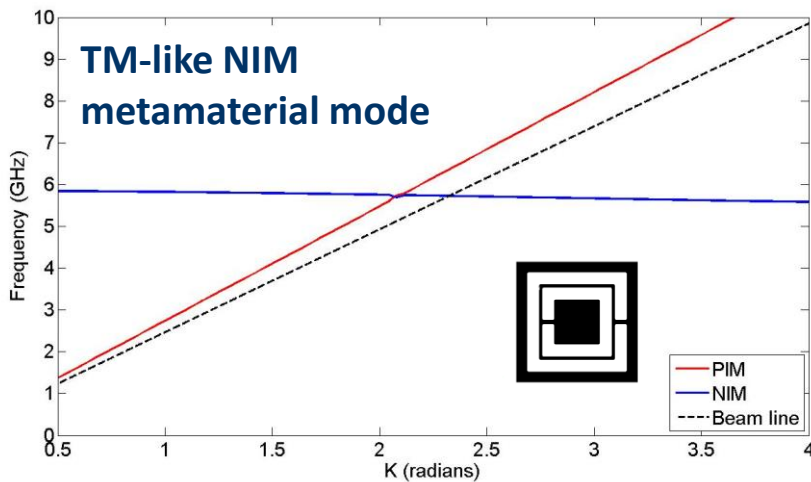
[M A Saphiro, *et al.*, *Proceedings of PAC09*, Vancouver, Canada (2009)]

# MTM-loaded waveguides



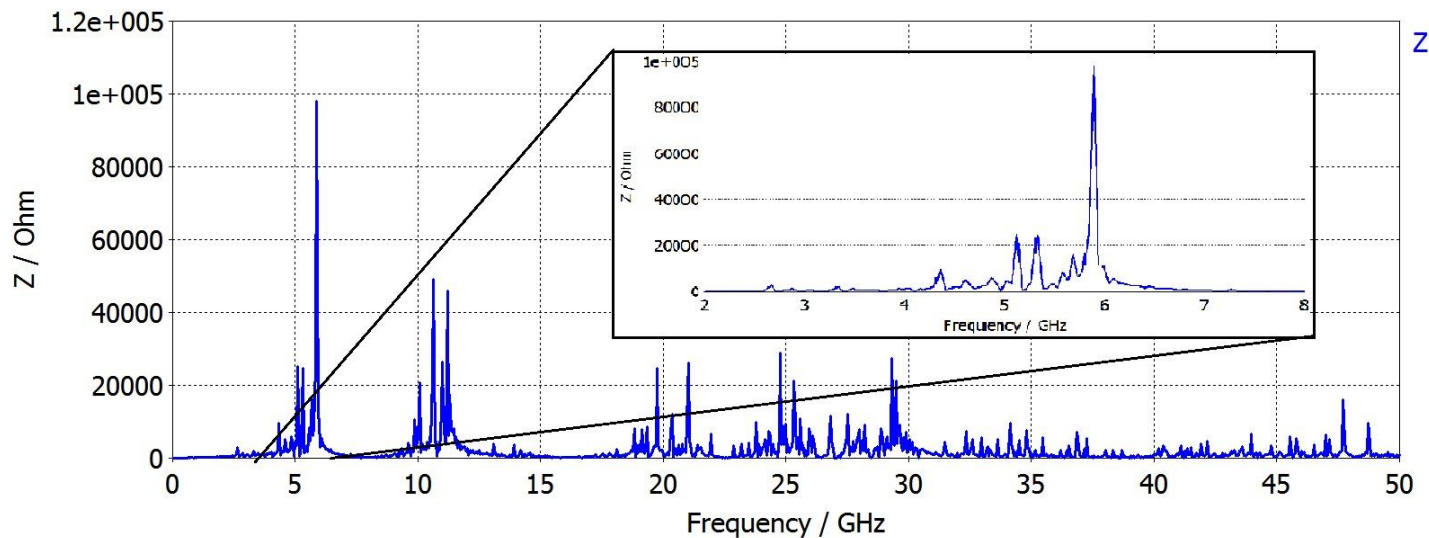
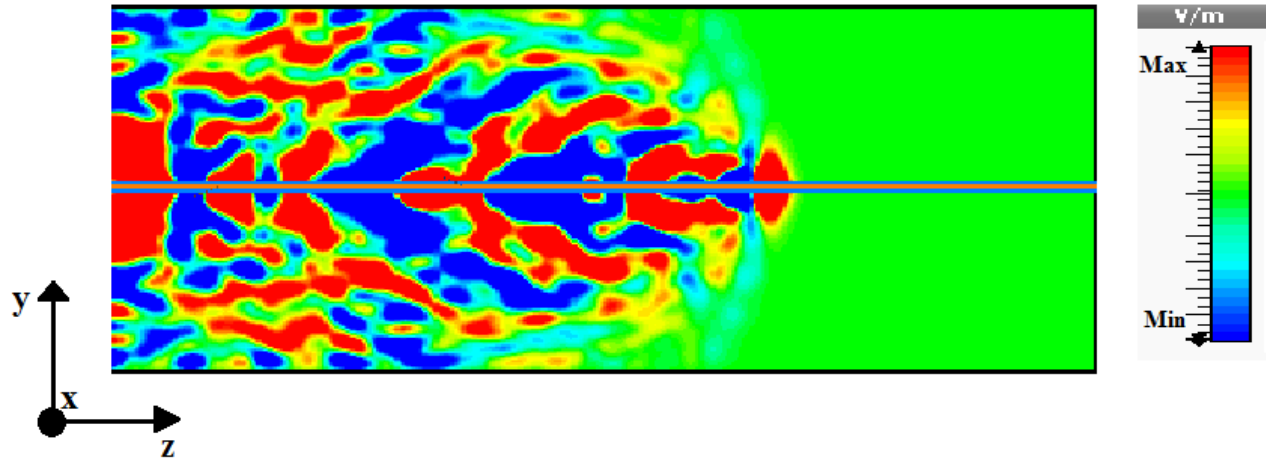
Width	8 mm
Outer ring slot length	6.6 mm
Slot width	0.8 mm
Inner ring slot length	4.6 mm
Split width	0.3 mm
Thickness	1 mm

- Long. Wake impedance = 55 k $\Omega$ /m, shunt impedance = 21 M $\Omega$ /m, R/Q = 4 k $\Omega$ /m



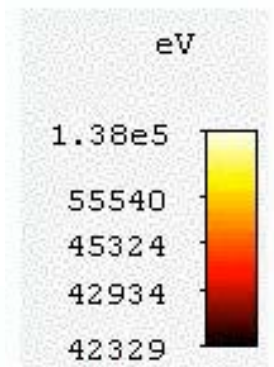
[E. Sharples, R. Letizia, *Journal of Instrumentation*, 2014 and *IEEE Trans. Plasma Science*, 2016]

# Wakefields simulations

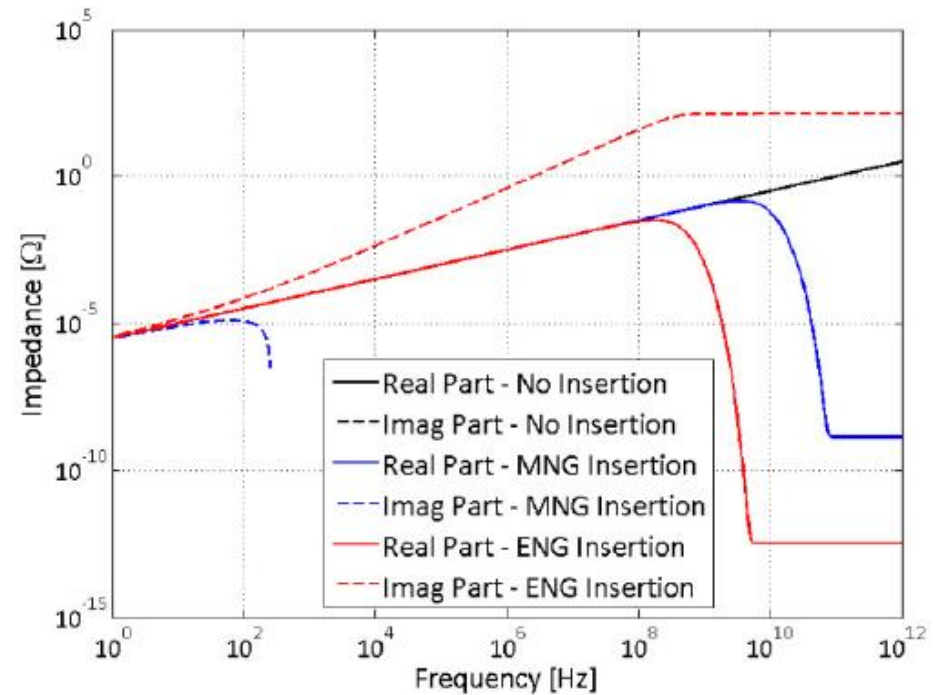
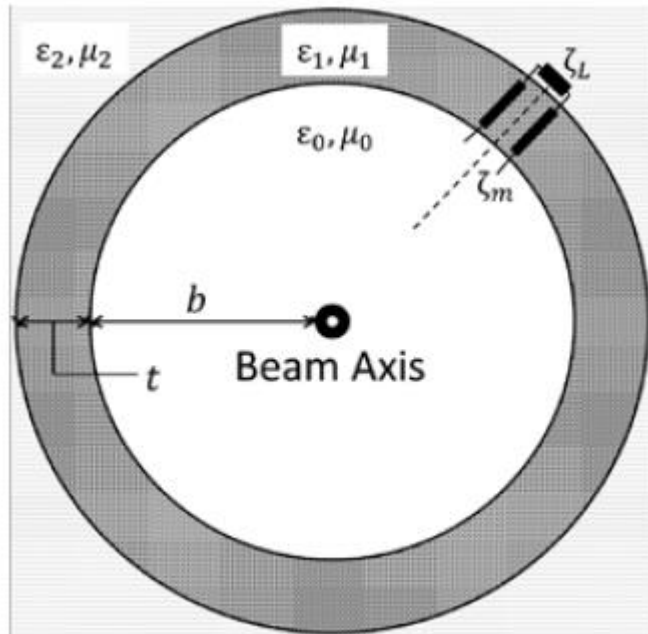


[E. Sharples, R. Letizia, *Journal of Instrumentation*, 2014  
and *IEEE Trans. Plasma Science*, 2016]

# Beam-wave interaction



# MTMs in accelerators studies



[A. Danisi et al., 2014]



# MTMs for high power applications

- Great need for designing MTMs tailored for high power applications
- MTMs are by nature narrowband → highly sensitive to changes in the material parameters and in their mechanical shapes due to thermal effects
- Another issue is the potential for breakdown induced by edge effects and high circulating currents in the metallic elements embedded in the background medium
- Choice of the geometry of the elements and the materials involved are central in the design of MTMs

# Characterisation

Which post-processing can be applied to obtain effective material parameters?

EM characterisation of different types of MTM is still a challenge.

Most known measurement techniques for linear EM characterisation of nano-structured layers and films:

Techniques	Measurement equipment	Direct results
Spectroscopy (optical range)	Precision spectrometer	Absolute values of S-parameters of a layer (film)
Interferometry (optical range)	Precision interferometer	Phase of S-parameters of a layer (film)
THz time domain spectrometry (optical range)	Detection of the phase change of THz wave passing through the MTM sample, compared to reference	Real and imaginary part of effective refractive index via phase measurements
Free space techniques (RF range)	Receiving antenna + vector network analyser	Complex S-parameters of the all set up between input and output ports
Waveguide techniques (RF range)	Receiving probe + vector network analyser	Complex S-parameters of the all set up between input and output ports

# Novel electromagnetic structures for high frequency acceleration (Part 5)

Rosa Letizia

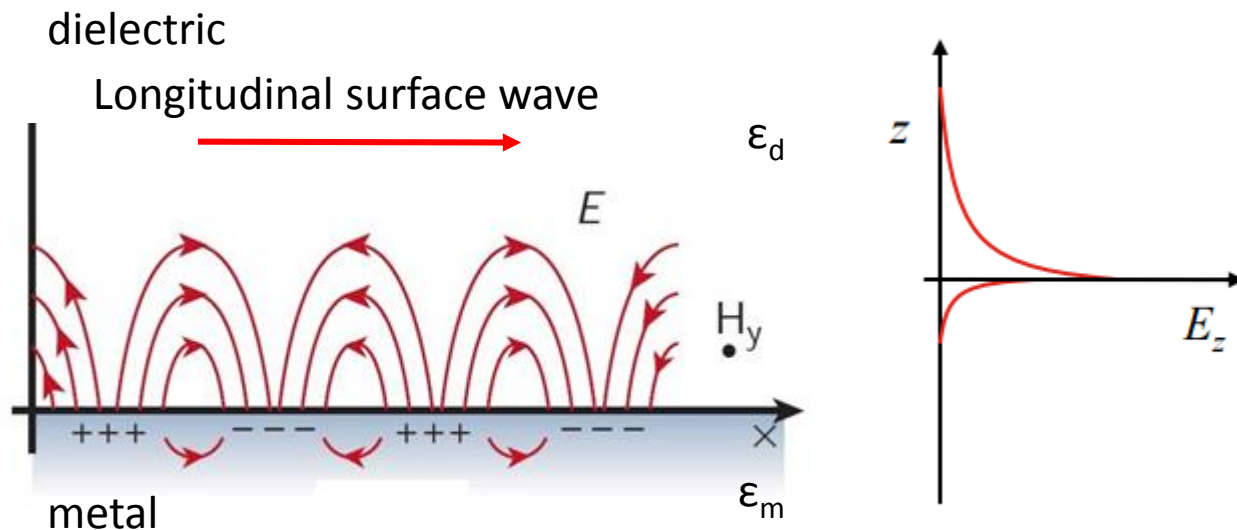
Lancaster University/ Cockcroft Institute

[r.letizia@lancaster.ac.uk](mailto:r.letizia@lancaster.ac.uk)

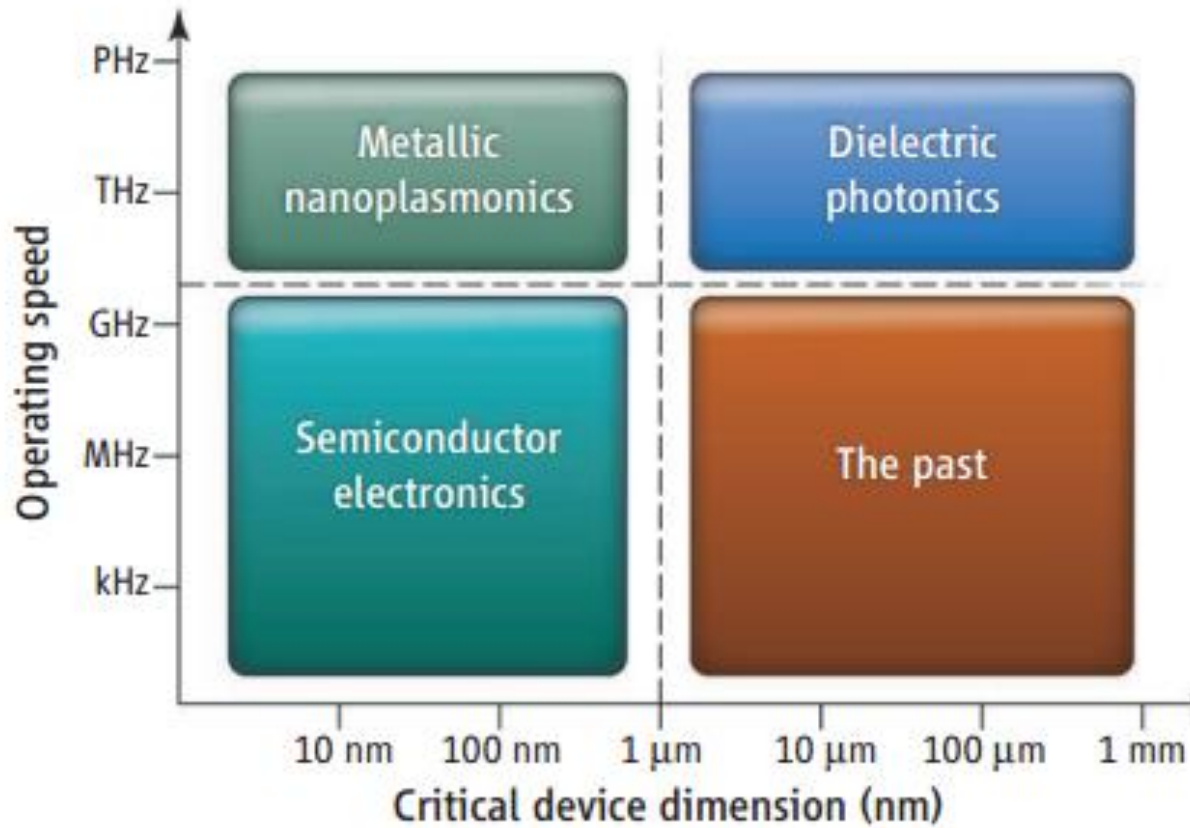
Cockcroft Institute, Spring term, 13/03/17

# Surface Plasmon Polariton wave

- Solutions of Maxwell equations for metal/dielectric interface
- Excitation of a coupled state between photons and plasma oscillations at the interface between a metal and a dielectric
- Perfectly flat surfaces support non-radiative (bound) SPPs, field on both sides is evanescent

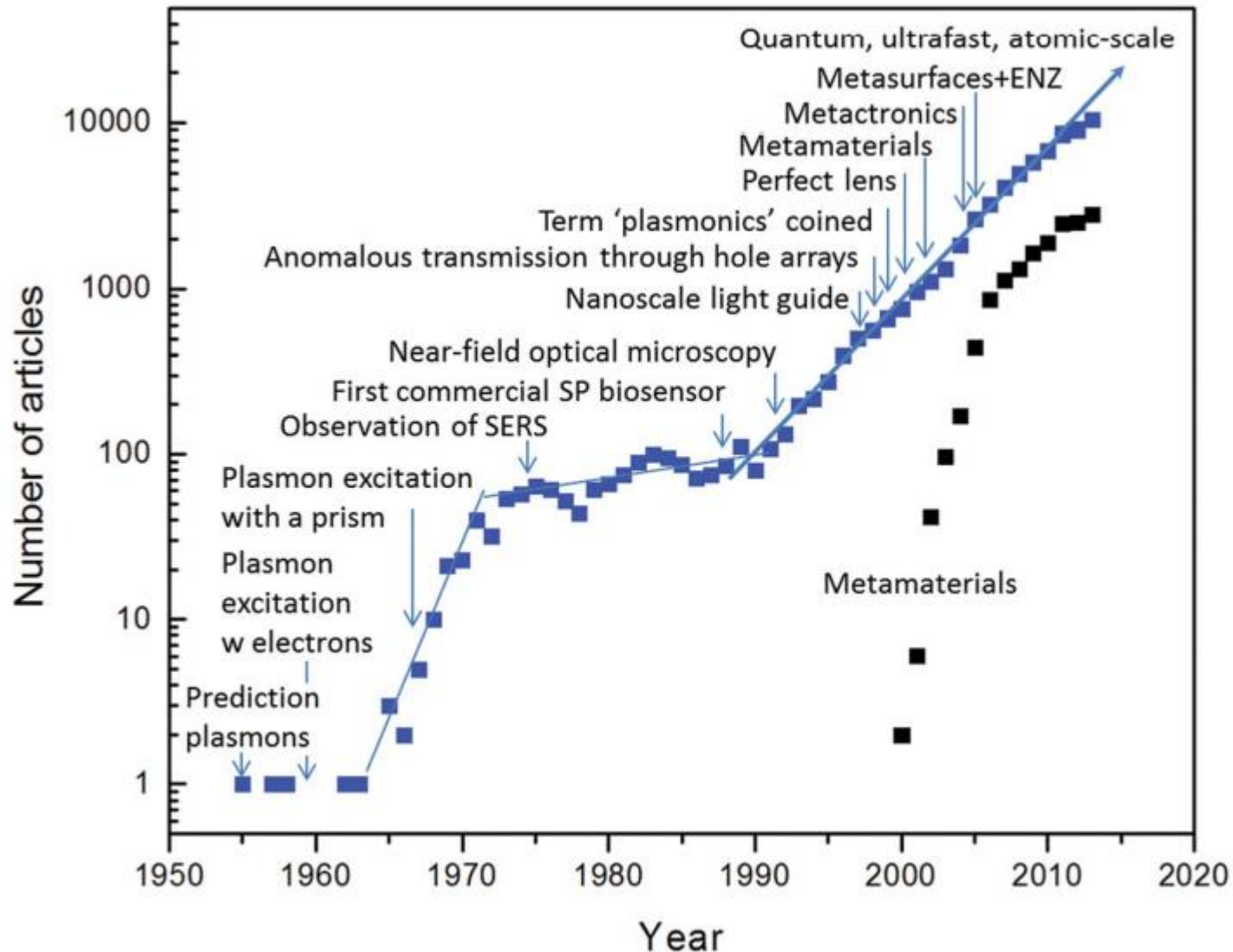


# Plasmonics



[M. L. Brongersma, and V. M. Shalaev, Science, 328 (2010)]

# Evolution of plasmonics



[M. L. Brongersma, Faraday Discuss., 178, 9 (2015)]

# Surface Plasmon Polaritons

- **Plasmon:** Elementary excitation.
- **Polaritons:** Coupled state between an elementary excitation and a photon.
- **Plasmon polariton:** coupled state between a plasmon and a photon.

- **Plasmons:**

- Free electrons in metal  $\rightarrow n \approx 10^{23} \text{ cm}^{-3}$
- Longitudinal density fluctuation (plasma oscillations) at frequency  $\omega_p$
- **Volume plasmon polariton**  $\rightarrow$  propagate through the volume for frequency for:

$$\omega > \omega_p$$

- **Surface plasmon polariton**  $\rightarrow$  propagate along a metal interface for:

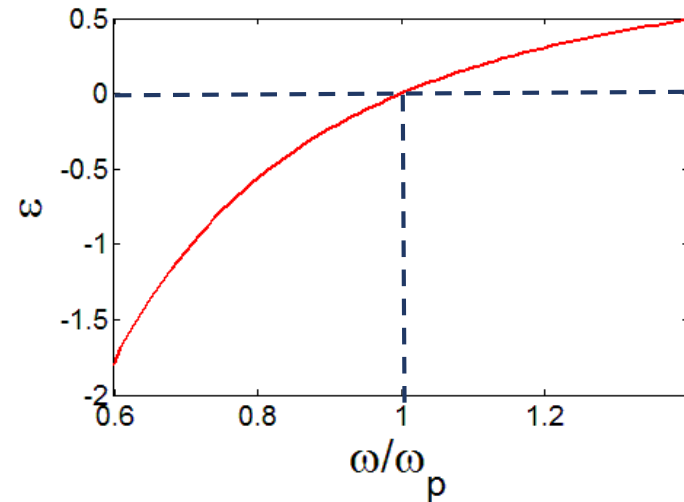
$$0 < \omega < \omega_p / \sqrt{2}$$

# Bulk plasmon in metals

Considering the metal as a free electron gas:

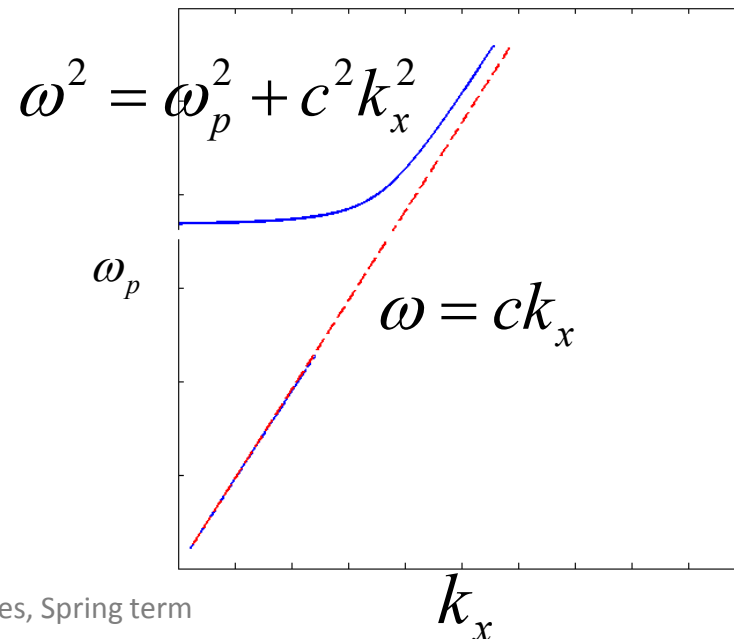
Drude model:  $\epsilon(\omega) = 1 - \left( \frac{\omega_p^2}{\omega^2} \right)$

$$\omega^2 \epsilon = c^2 k^2$$



Dispersion relation for EM waves in the electron gas (volume or bulk plasmons):

$$\omega^2 - \omega_p^2 = c^2 k^2$$



Only modes for:  $\omega > \omega_p$



# SPP dispersion

$$E_y = 0$$

$$H_x = H_z = 0$$

$$H_d = (0, H_{yd}, 0)e^{i(k_{xd}x + k_{zd}z - \omega t)}$$

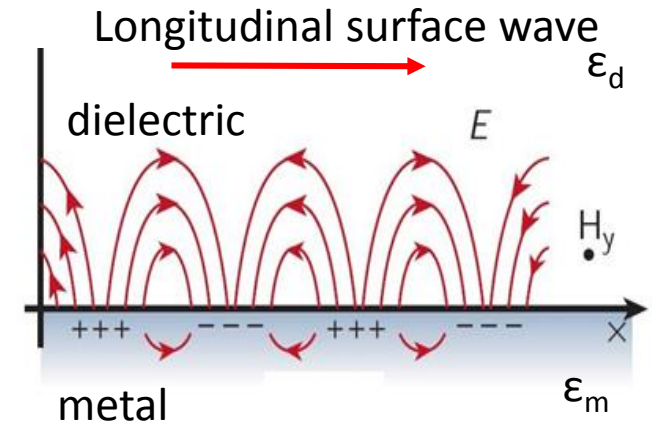
$$E_d = (E_{xd}, 0, E_{zd})e^{i(k_{xd}x + k_{zd}z - \omega t)}$$

$z > 0$

$$H_m = (0, H_{ym}, 0)e^{i(k_{xm}x + k_{zm}z - \omega t)}$$

$$E_m = (E_{xm}, 0, E_{zm})e^{i(k_{xm}x + k_{zm}z - \omega t)}$$

$z < 0$




$$z=0 \left\{ \begin{array}{l} \epsilon_m E_{zm} = \epsilon_d E_{zd} \\ E_{xm} = E_{xd} \\ H_{ym} = H_{yd} \end{array} \right\} k_{xm} = k_{xd}$$

## SPP dispersion

$$k_{zi} H_{yi} = -\omega \varepsilon_i E_{xi} \Rightarrow \begin{cases} k_{zm} H_{ym} = -\omega \varepsilon_m E_{xm} \\ k_{zd} H_{yd} = -\omega \varepsilon_d E_{xd} \\ E_{xm} = E_{xd} \\ H_{ym} = H_{yd} \end{cases}$$

$$\frac{k_{zm}}{\varepsilon_m} H_{ym} = \frac{k_{zd}}{\varepsilon_d} H_{yd}$$



$$\frac{k_{zm}}{\varepsilon_m} = \frac{k_{zd}}{\varepsilon_d} \quad (1)$$

Condition for the SP to exist

Considering that for any EM wave:

$$k_x^2 + k_{zi}^2 = \varepsilon_i \left( \frac{\omega}{c} \right)^2 \quad \Rightarrow \quad k_{SP} = \sqrt{\varepsilon_i \left( \frac{\omega}{c} \right)^2 - k_{zi}^2} \quad (2)$$

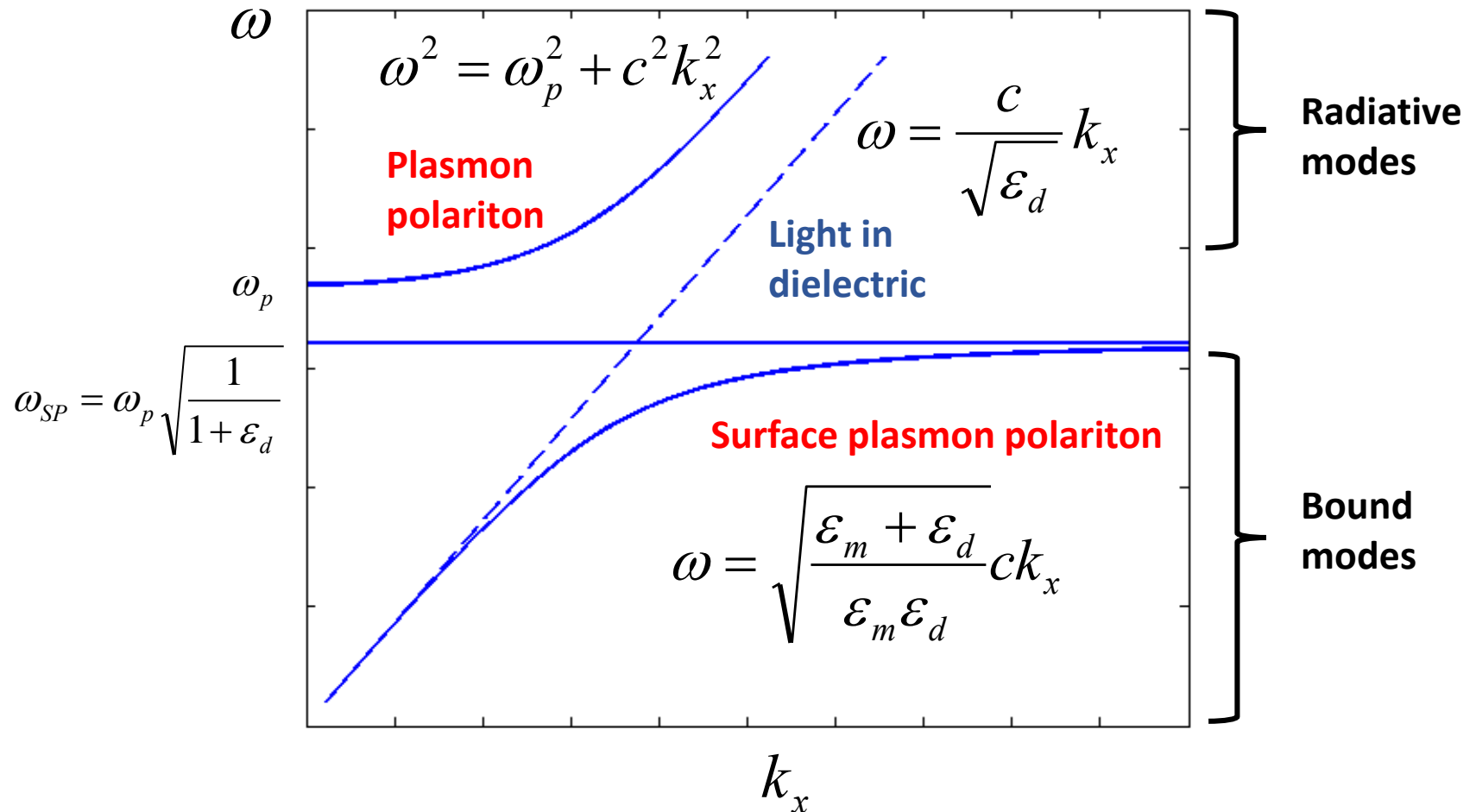
Thus using (1) and (2):

$$k_{SP} = \frac{\omega}{c} \sqrt{\frac{\varepsilon_m \varepsilon_d}{\varepsilon_m + \varepsilon_d}}$$

Dispersion relation

# Surface Plasmon modes

Optical frequencies with small  $\lambda_{SP} \rightarrow$  Sub-wavelength confinement



# Drude-like materials

- ***Noble metals (Ag, Au, Cu, Al ...)***
  - Plasma frequency in the UV range
  - Applications from visible range to the mid-IR
  - M. A. Ordal et al., Appl. Opt., 22, 7 (1983)
- ***Doped silicon***
  - Plasma frequency in the IR range
  - J. C. Ginn et al., J. Appl. Phys. 110, 4, (2011)
- ***Oxides and nitrides***
  - Oxides: near-IR range
  - Transition metal nitrides (TiN): visible range
  - G. V. Naik et al., Opt. Material Express, 1, 6, (2011)
- ***Graphene***
  - IR frequency range
  - A. Vakil and N. Engheta, Science, 332, 6035 (2011)

# SPP propagation length

$$k_{spp} = k'_x + ik''_x = \frac{\omega}{c} \sqrt{\frac{\epsilon_m}{\epsilon_m + 1}}$$

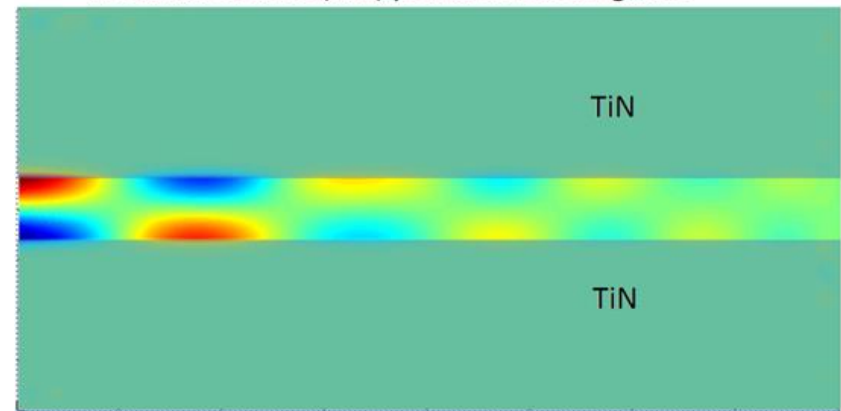
Considering lossy Drude model for metal:

$$\epsilon(\omega) = 1 - \left( \frac{\omega_p^2}{\omega^2 + i\gamma\omega} \right)$$

**Propagation  
Length**

$$L_x = \frac{1}{2k''_x}$$

Titanium Nitrate (TiN) plasmonic waveguide



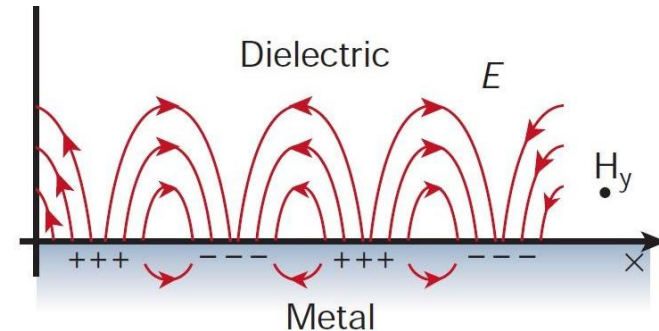
# Excitation of Surface Plasmon modes

## How to couple light to SPPs?

$$k_{spp} < k_x^{photon}$$

Different techniques are possible:

- High energy electrons
- Kretschman geometry
- Otto configuration
- Gratings
- Nanoslits
- ...

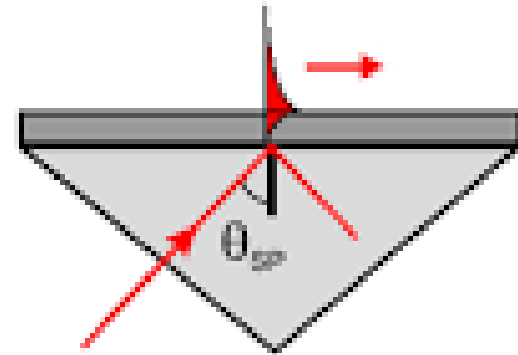


## Kretschmann geometry

*SPPs at a metal/air interface can be excited from a high refractive index medium*

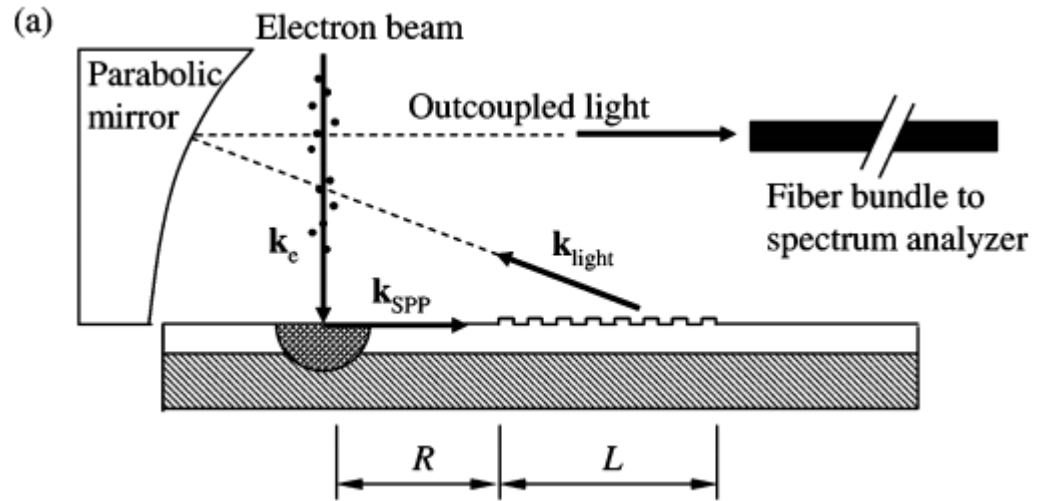
$$k_{high} > k_{SPP}$$

- SiO<sub>2</sub> prism creates evanescent wave by total internal reflection.
- Strong coupling between parallel component of  $k_{high}$  and  $k_{SPP}$ .
- Reflected wave reduced in intensity indicate coupling with SPP.
- SPPs at the metal/glass interface cannot be excited.

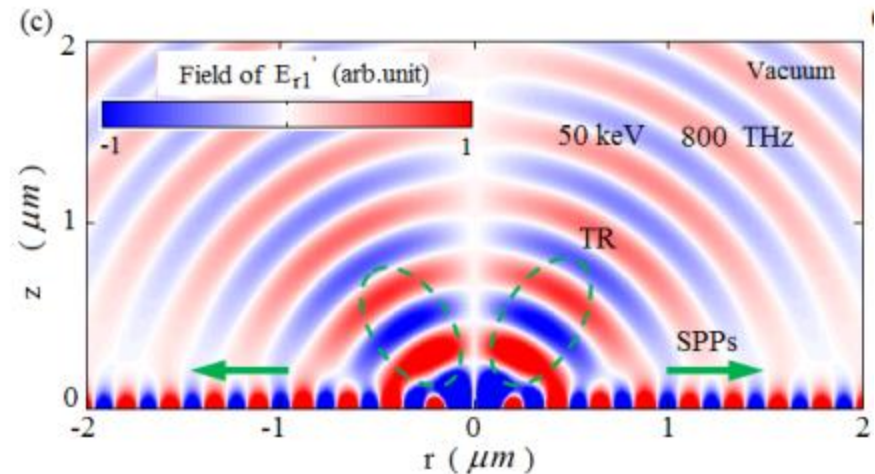
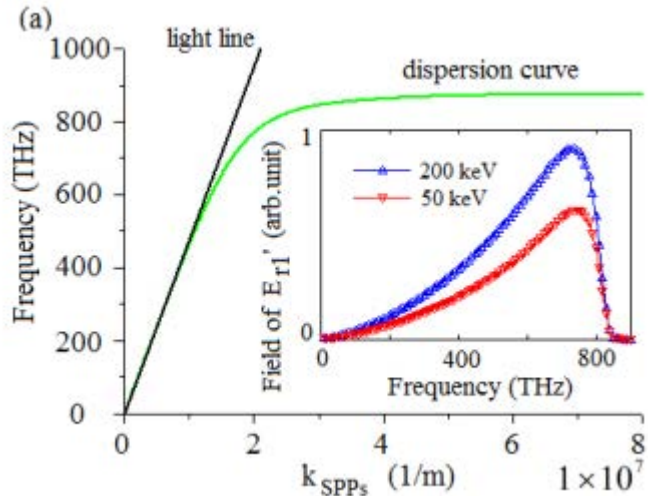
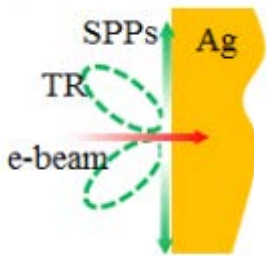


# Beam excitation of Surface Plasmon modes

- Predicted by **Ritchie**, Phys. Rev. **1957**, 106 (5), 874-881, SPP modes can be excited by *perpendicular* electron beam (50 keV)



[M. V. Bashevov et al., *Nano Letts*, (2006)]

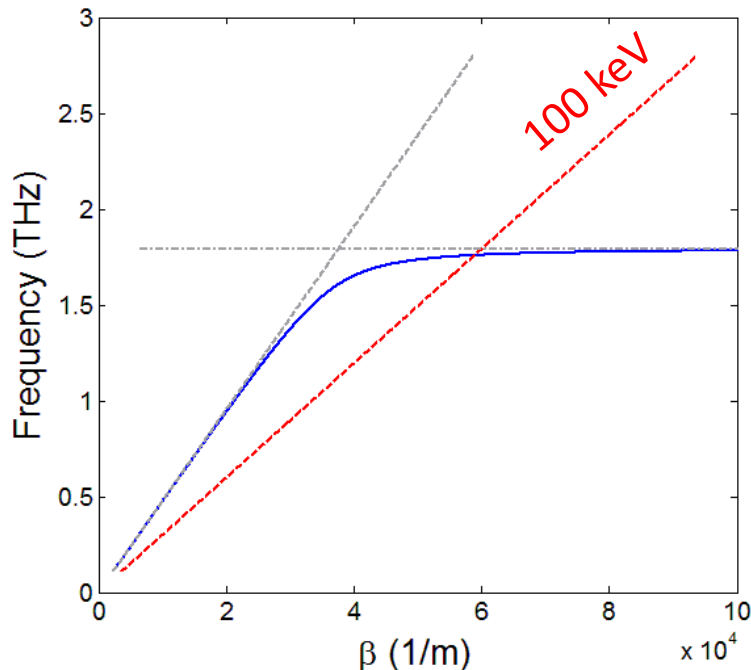
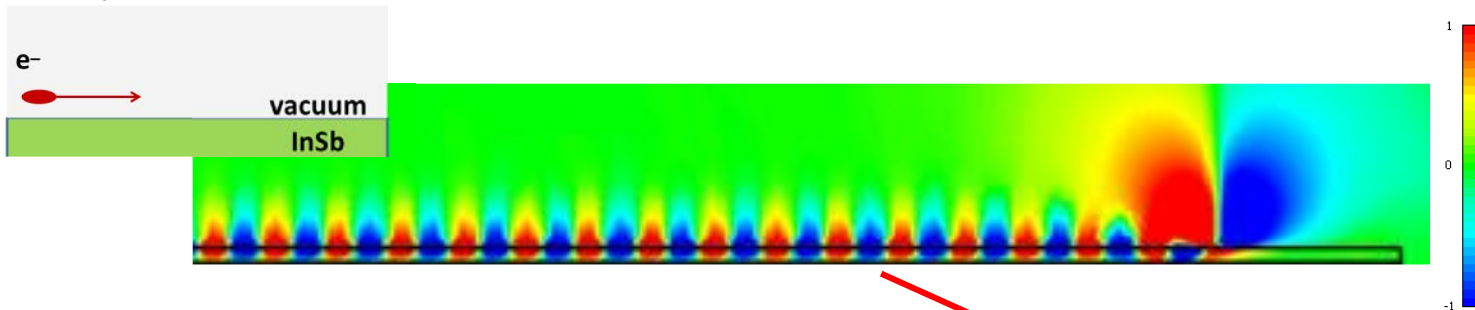


[S. Gong et al., *Optics Express*, (2014)]



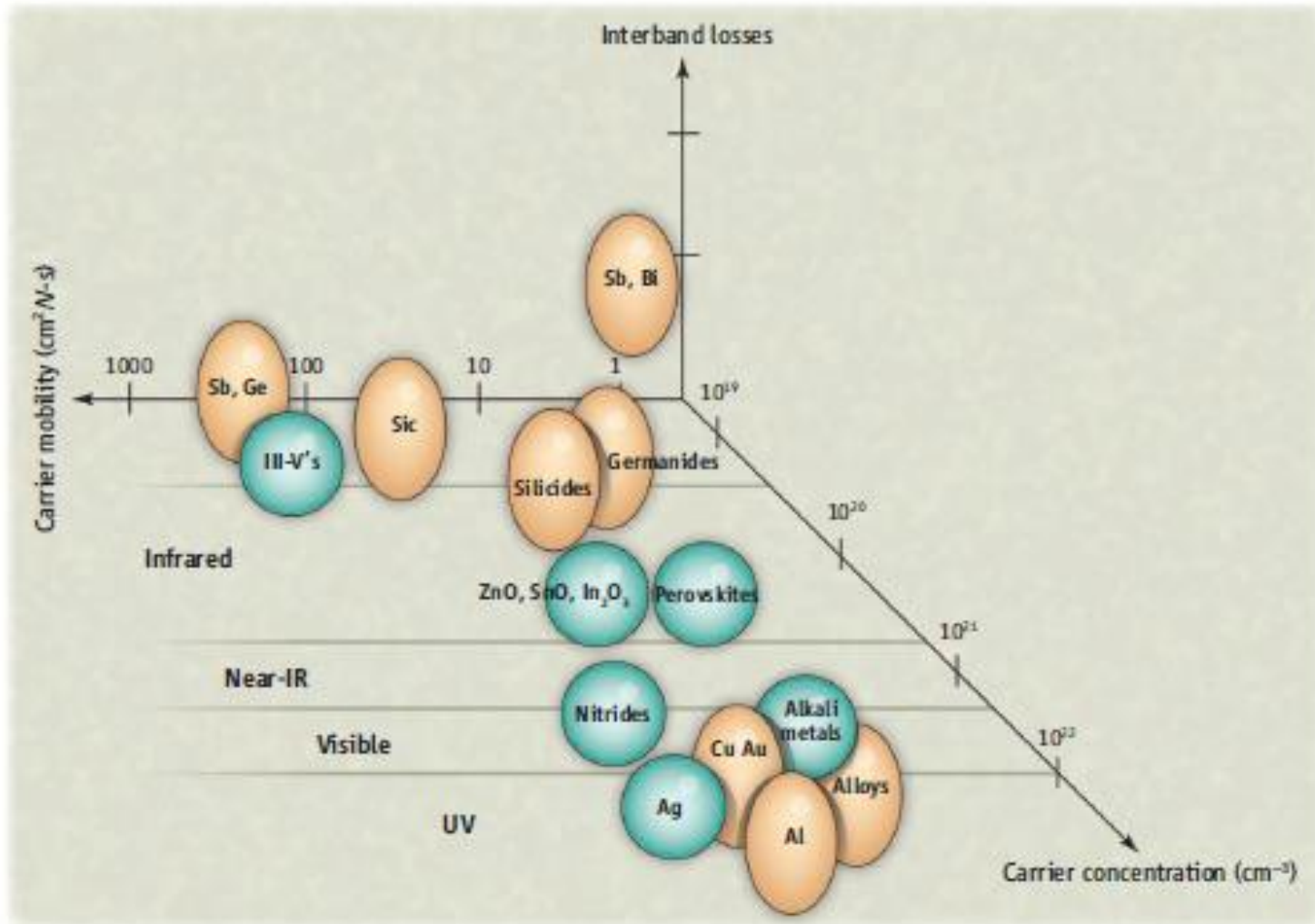
# Beam excitation of Surface Plasmon modes

- SPP modes can also be excited by *parallel* electron beam
- Example: 100 keV electron bunch



Considering contribution of losses, SPPs decay within the propagation length

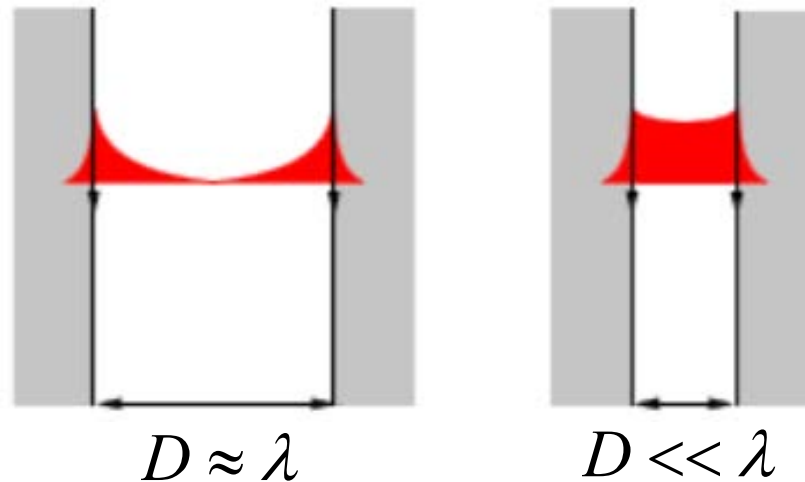
# Tunability of plasmonic properties



[A. Boltasseva and H. Atwater, *Science*, 331, (2011)]

## Metal-Insulator-Metal plasmonic waveguide

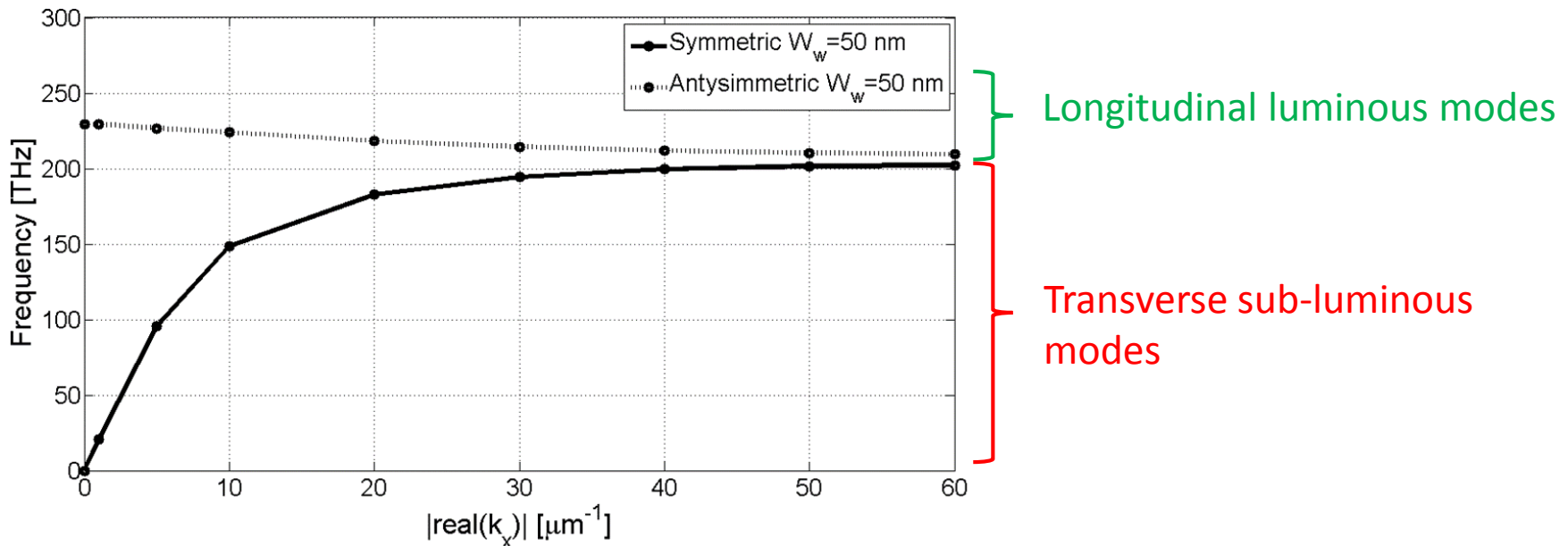
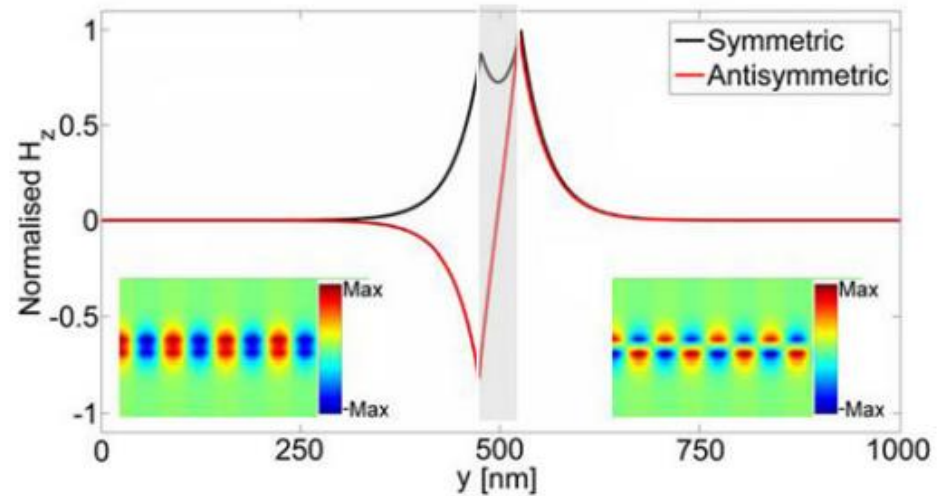
- Similarly to the case of the open grating, a single interface does not support luminous phase velocities ( $v_{ph} = \omega/k_x = c$ ).
- Coupling of the SPP modes from the two single interfaces  $\rightarrow$  tri-layer system.



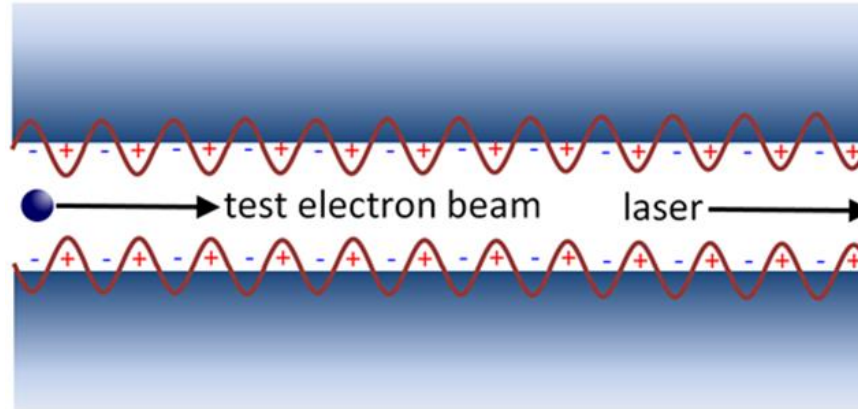
- Sub-wavelength propagation  $\rightarrow$  MIM and IMI plasmonic waveguides.
- Miniaturisation of conventional optical waveguides.

# Symmetric and antisymmetric SPP modes

- Accelerating modes for relativistic beams are found coupling two interfaces in the metal-insulator-metal configuration.

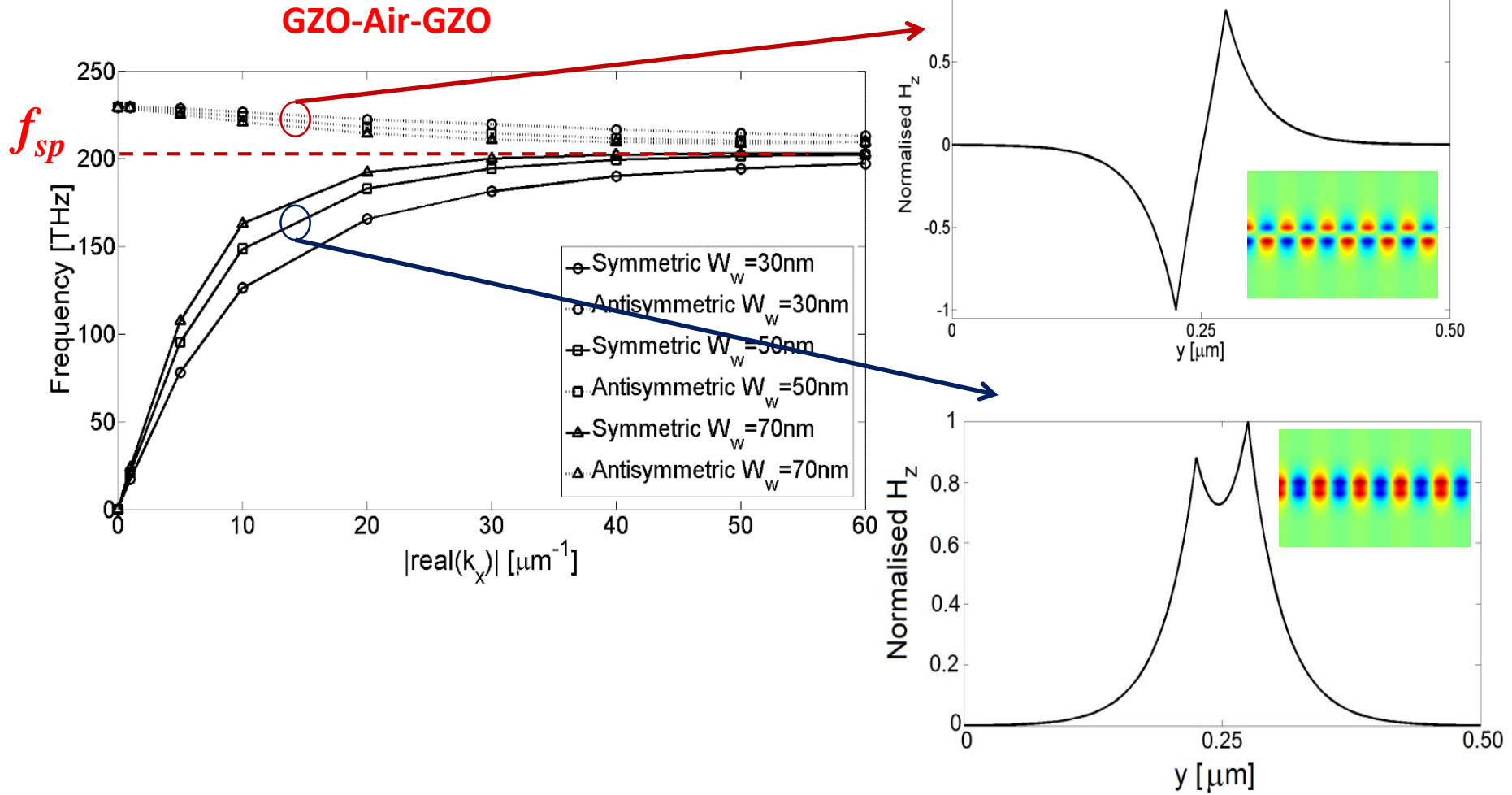


# Surface wave accelerators?



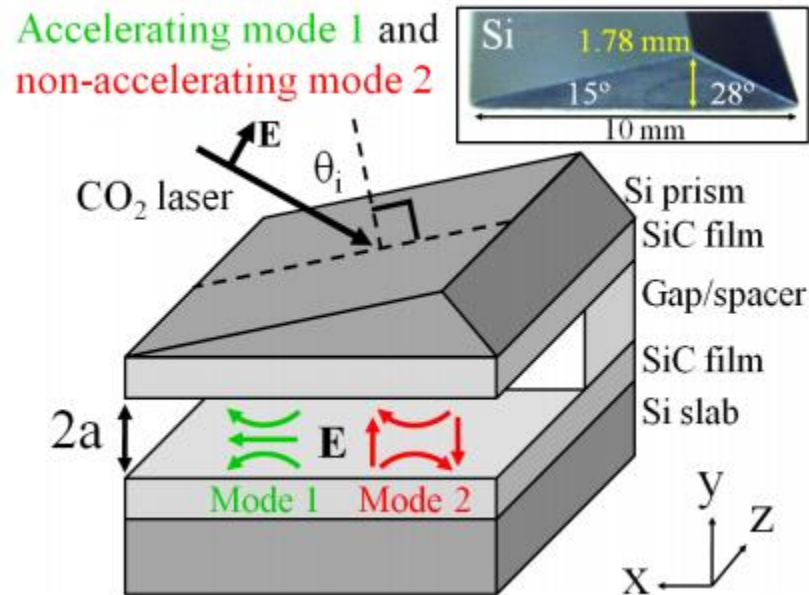
- **Properties:**
- Metal or Drude-like material
- Plasmonic resonances make metal suitable at very high frequencies
- Easy fabrication
- Narrow gap (maximises the  $E_{acc} / E_{\perp}$ )
- Dispersion engineering
- Tunable via material properties

# Surface wave accelerators?



[R. Letizia, D. Pinto, *IEEE Journal of Lightwave Technology*, (2014)]

# IR-range surface wave accelerator (Shvets 2012)

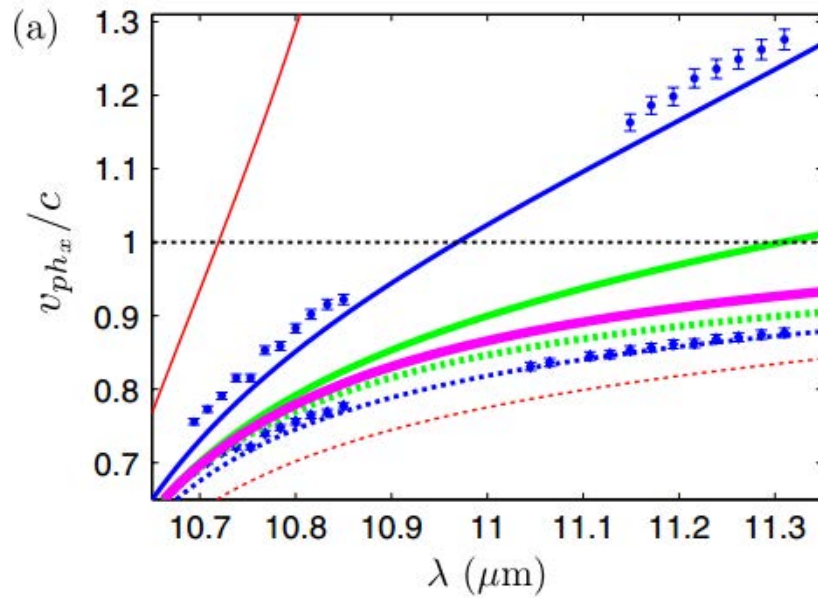


## Silicon carbide:

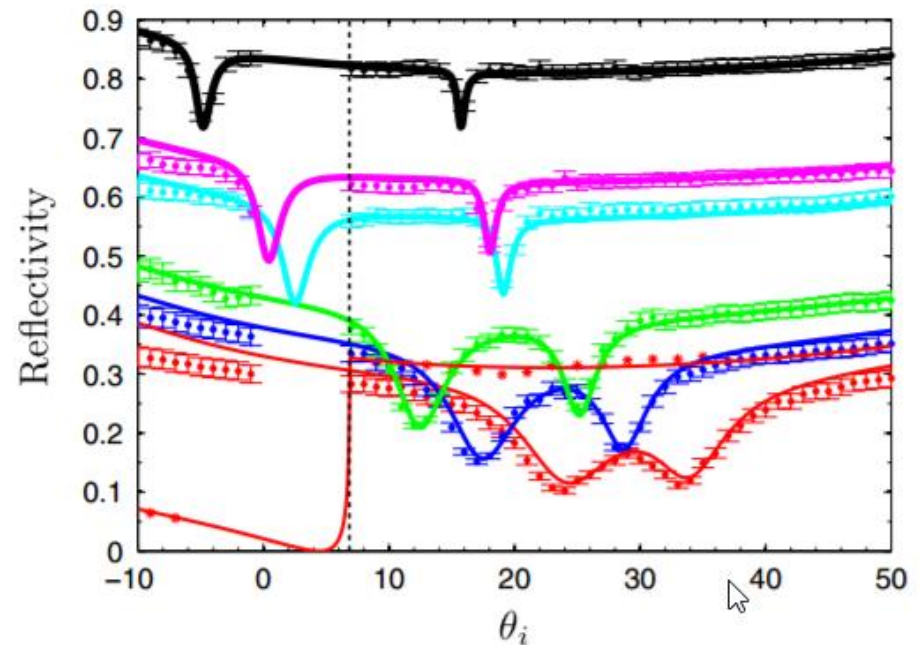
- Negative dielectric constant in mid-IR range
- Compatible with short pulse high power CO<sub>2</sub> lasers at  $9.6 \mu\text{m} < \lambda < 11.3 \mu\text{m}$
- Operation in hostile and high temperature environment ( $>1000^\circ \text{C}$ )
- High electrical breakdown (DC threshold  $\sim 300 \text{ MV/m}$ )

[Neuner et al., *PR-STAB*, 15, 031302 (2012)]

# IR-range surface wave accelerator (Shvets 2012)



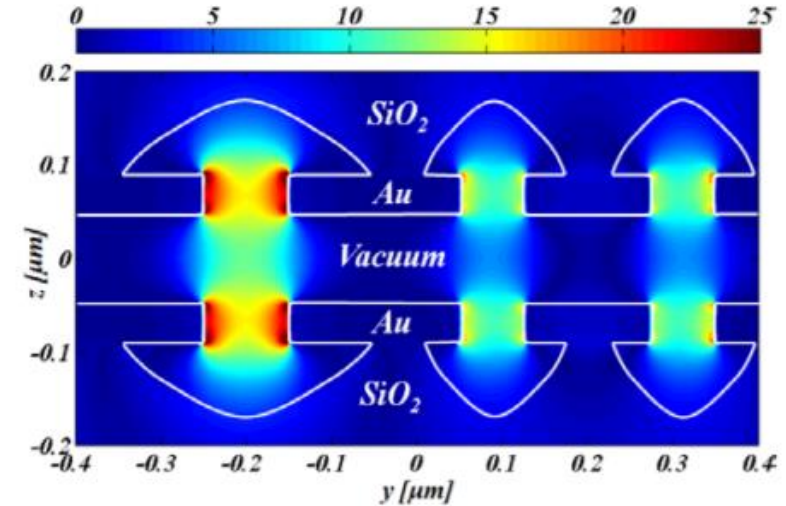
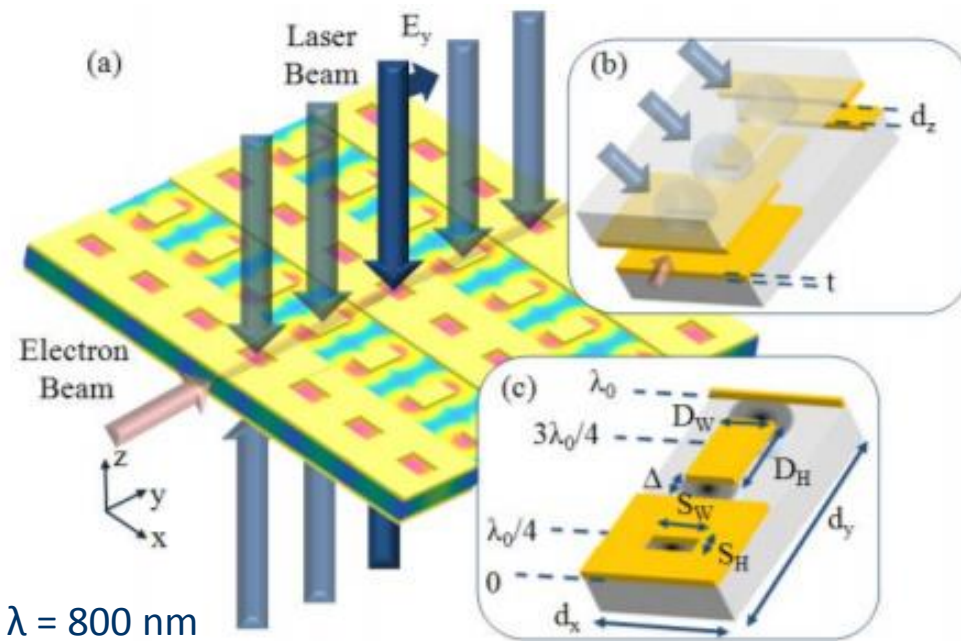
Shift of  $\lambda$  luminous of longitudinal mode (solid line) as gap size increases



[Neuner et al., *PR-STAB*, 15, 031302 (2012)]



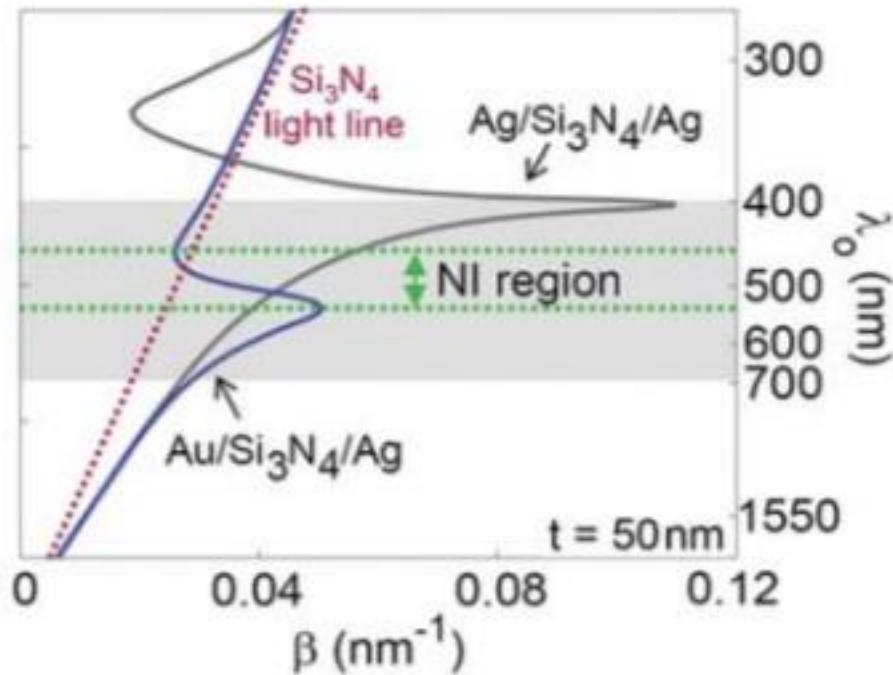
# Plasmonic metasurface (Bar-Lev/Scheuer 2014)



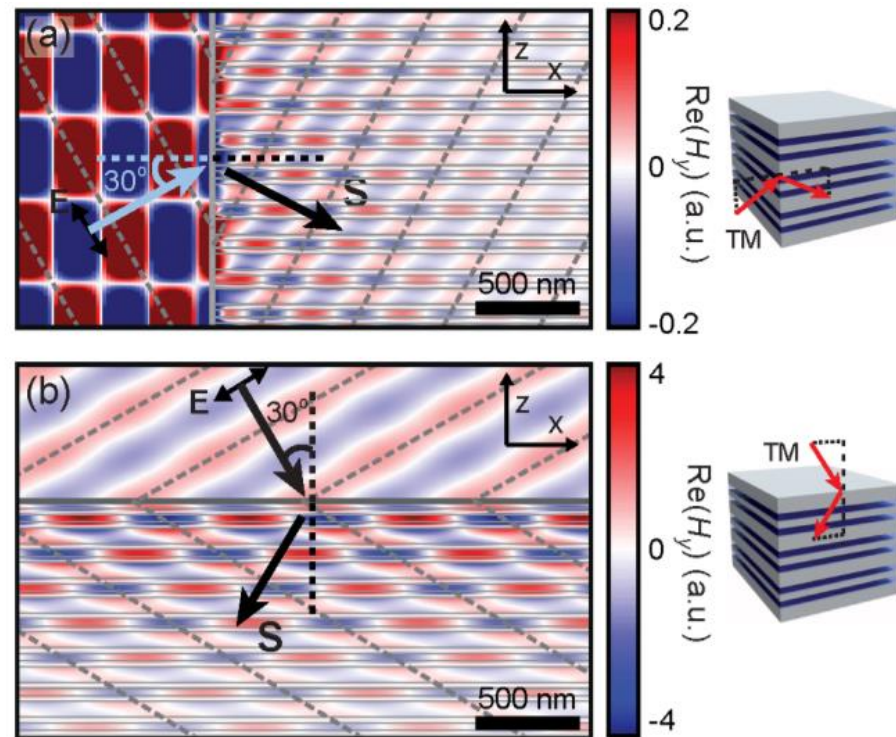
Laser driven plasmonic metasurface-based particle acceleration:

- Plasmonic nanoantennas to enhance EM energy concentration in a small volume  $\rightarrow$  large enhancement of the local field
- Combination of resonant structure (metasurface) with ultra-short pulse operation
- Under symmetrical excitation,  $G = 2.64 E_0$
- Au films on dielectric substrate can attain similar damage threshold than  $\text{SiO}_2$  under fs pulses.
- Max unloaded gradient estimated as 4.64 GV/m for 100 fs pulses (higher for shorter pulses).

# Plasmonic approach to negative refraction



Coupling of MIM waveguides, isotropic negative refraction of TM waves.



[Lezec et al., *Science*, **316**, (2007)]

[Verhagen et al., *Phys Rev Letts*, **105** (2010)]

# Novel electromagnetic structures for high frequency acceleration (Part 6)

Rosa Letizia

Lancaster University/ Cockcroft Institute

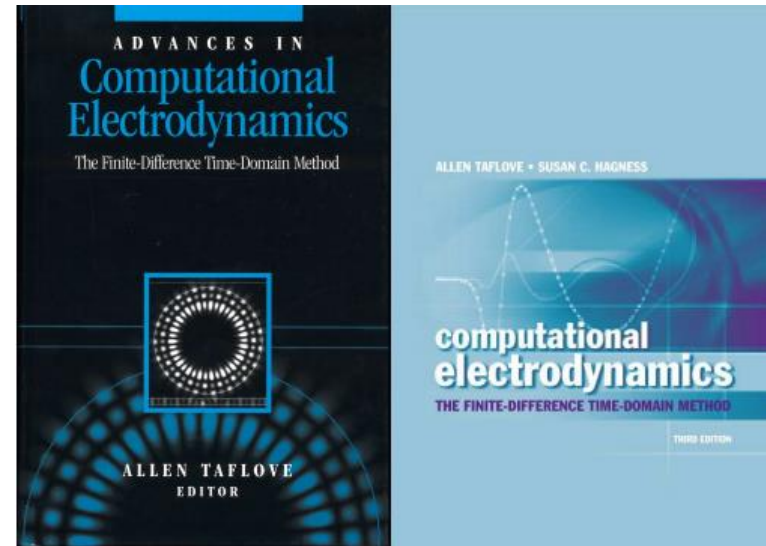
[r.letizia@lancaster.ac.uk](mailto:r.letizia@lancaster.ac.uk)

Cockcroft Institute, Spring term, 13/03/17

# Modelling – Finite Difference Time Domain

## Allen Taflove, 1998

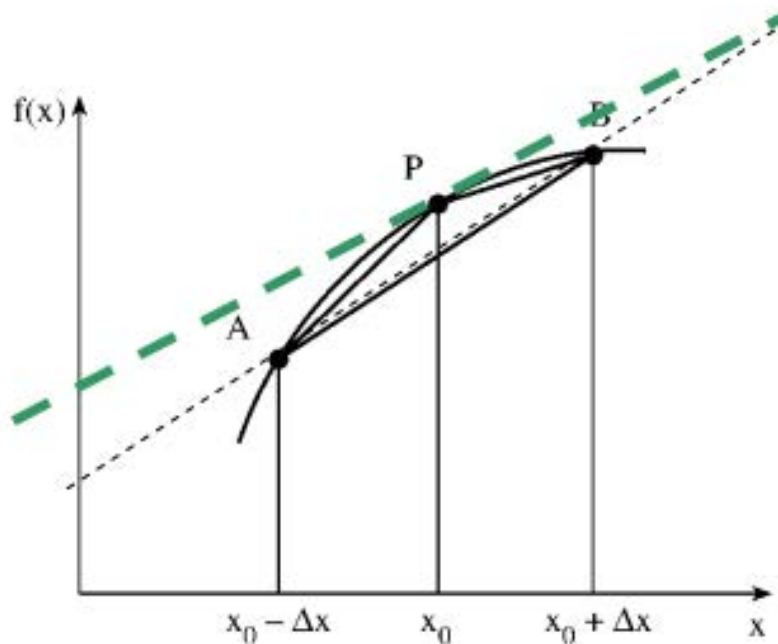
- The most common method for the simulation of optical and microwave devices.
- It relies on the finite difference formulation in order to calculate derivatives in space and in time.
- It can handle a wide variety of photonic and microwave devices.
- Its formulation is relatively simple and adapts well on parallel processing
- Simulation time can be long because of the maximum limit imposed to the time step.



## General steps of time domain modelling

- Develop time-dependent integral or Maxwell's curl equations.
- Discretise the equations in space and in time by means of an appropriate grid in space, and suitable basis and testing functions.
- Derive a set of equations that relate unknown with known quantities (starting from an initial value that usually is given by the source field).
- Generate a numerical solution of this initial-value problem in space and time.

## Central difference scheme (1D case)



$$f'(x_0) \cong \frac{f(x_0 + \Delta x) - f(x_0 - \Delta x)}{2\Delta x}$$

If spatial derivatives are approximated by trigonometric functions Chebyshev polynomials, then we obtain Pseudospectral Time Domain method (PSTD – Liu, 1997)

## Finite Difference Time Domain (FDTD)

### Maxwell's equations

$$\nabla \times \bar{H} = \frac{\partial \bar{D}}{\partial t} + \bar{J}$$

$$\nabla \times \bar{E} = -\frac{\partial \bar{B}}{\partial t}$$

$$\nabla \cdot \bar{D} = 0$$

$$\nabla \cdot \bar{B} = 0$$

$$\bar{D} = \varepsilon_0 \varepsilon \bar{E}$$

$$\bar{B} = \mu_0 \mu \bar{H}$$

$$\begin{cases} \bar{E}(\bar{r}, t) \rightarrow E_y(\bar{x}, t) \\ \bar{H}(\bar{r}, t) \rightarrow H_z(\bar{x}, t) \end{cases}$$

TEM wave

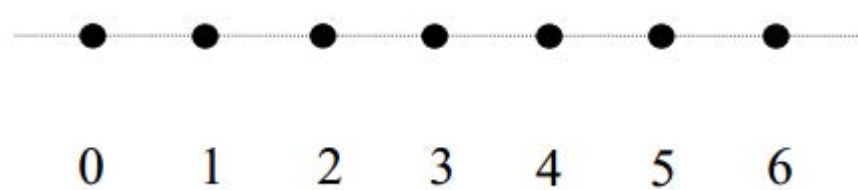
$$E_y, H_z$$

$$\begin{cases} \frac{\partial H_z(t)}{\partial t} = -\frac{1}{\mu_0 \mu} \frac{\partial E_y}{\partial x} \\ \frac{\partial E_y(t)}{\partial t} = \frac{1}{\varepsilon_0 \varepsilon} \frac{\partial H_z}{\partial x} \end{cases}$$

\*A. Taflove, and S. C. Hagness, *Computational Electrodynamics: the finite-difference time-domain method*, Artech House, 2005

# Finite differences

Uniform grid:  $\{x_i\}$



$$x_i = i$$

$$h, i = 0, 1, 2, \dots$$

$$u_i = u(x_i)$$

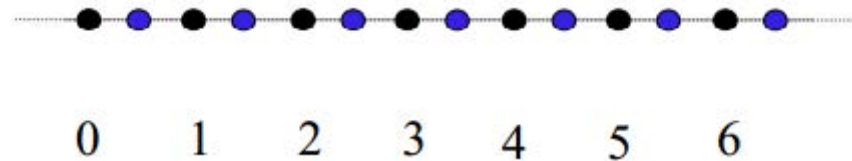
$$\frac{du_i}{dx} = \frac{u_{i+1} - u_i}{h} + O(h) = D^+ u_i + O(h)$$

$$\frac{du_i}{dx} = \frac{u_i - u_{i-1}}{h} + O(h) = D^- u_i + O(h)$$

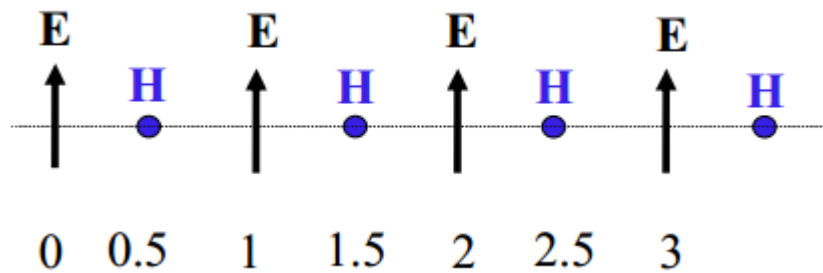
$$\frac{du_i}{dx} = \frac{u_{i+1} - u_{i-1}}{2h} + O(2h)^2 = D^c u_i + O(2h)^2$$



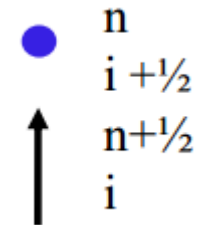
# Staggering and leapfrogging



- E field
- H field

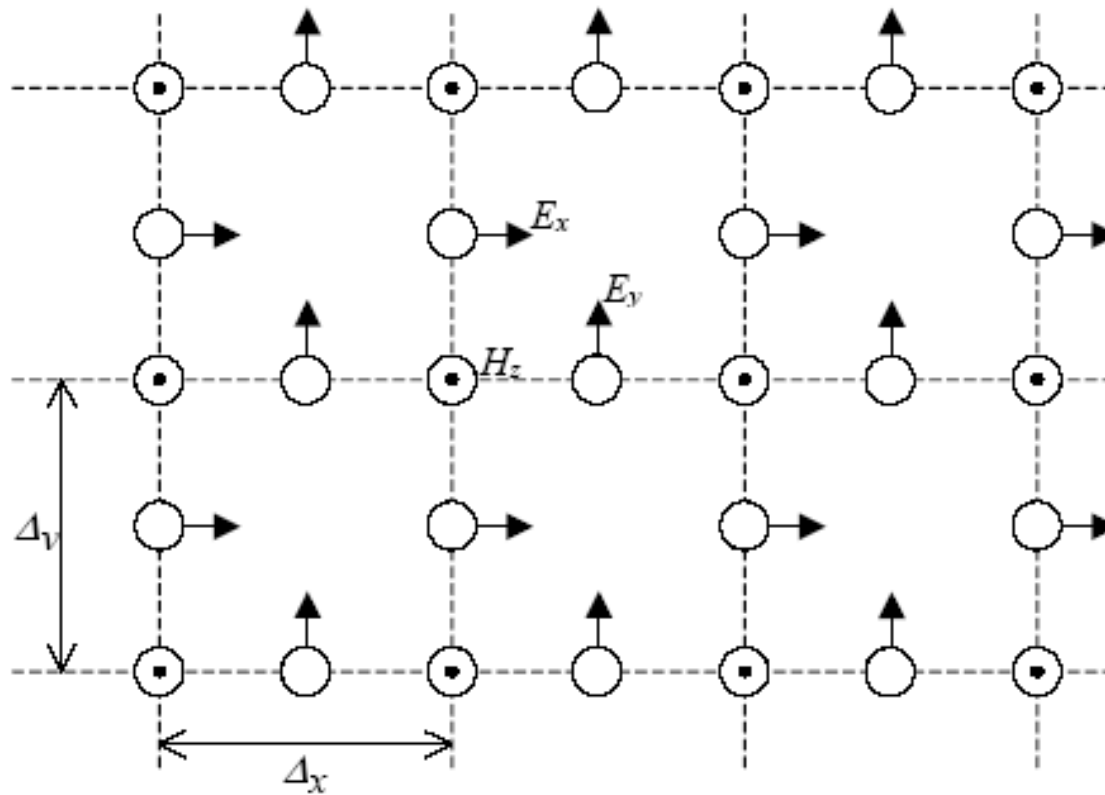


Marching of the fields:



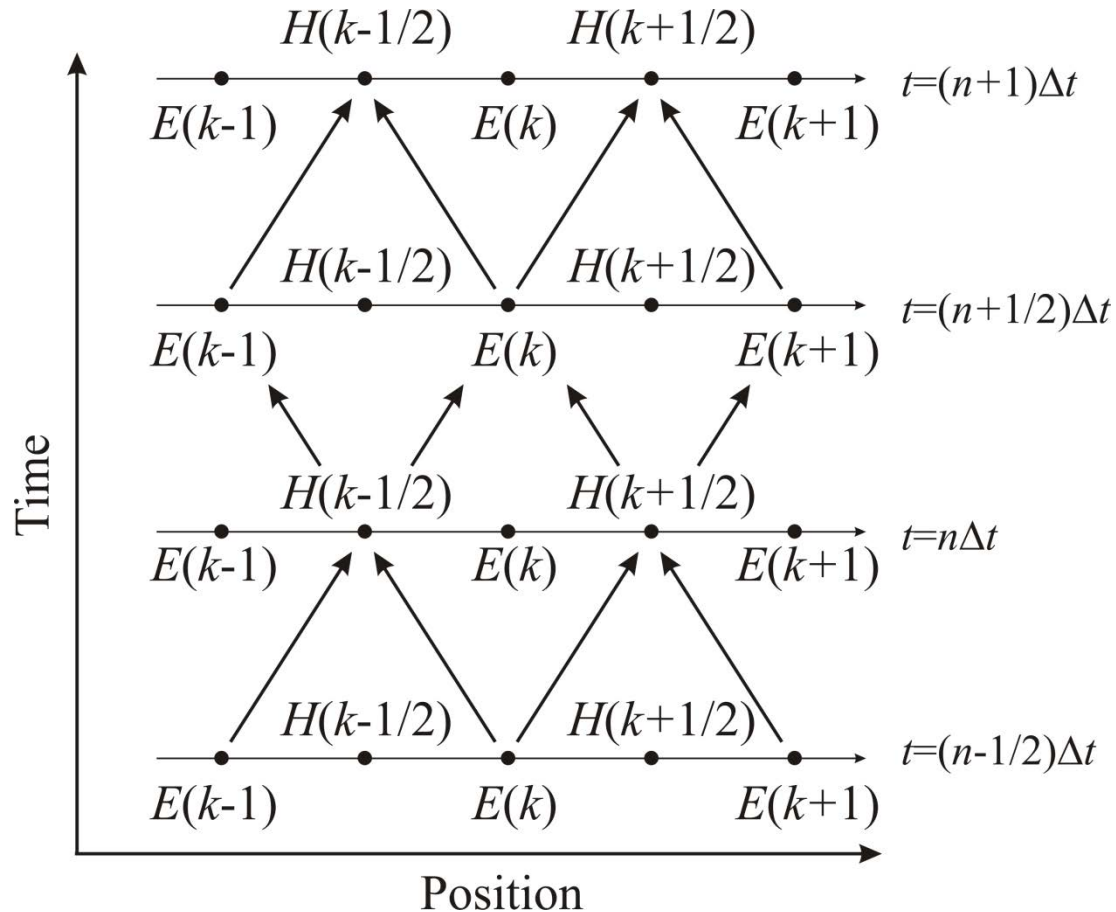
# Yee Algorithm

Discretisation in space is performed on the Yee's cell:



# Leapfrog scheme

Discretisation in time is obtained following the leapfrog arrangement\*:



# 2D-FDTD formulation

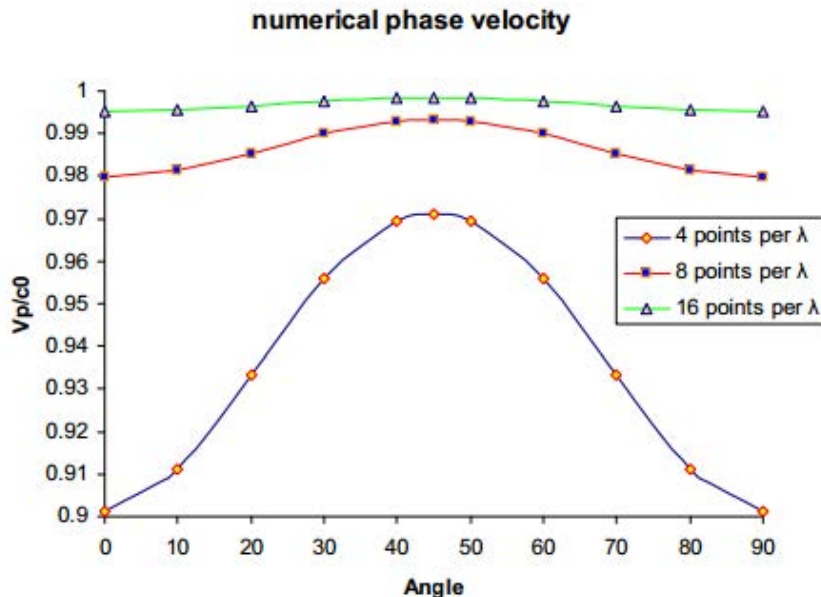
Applying Yee's cell and leapfrog arrangement to Maxwell's equations  
a set of discretised equations are derived (2-dimension TE mode)

$$\left\{ \begin{array}{l} H_x \Big|_{i-1/2, j+1}^{n+1/2} = H_x \Big|_{i-1/2, j+1}^{n-1/2} + \frac{\Delta t}{\mu} \left( \frac{E_y \Big|_{i-1/2, j+3/2}^n - E_y \Big|_{i-1/2, j+1/2}^n}{\Delta z} \right) \\ H_z \Big|_{i+1, j-1/2}^{n+1/2} = H_z \Big|_{i+1, j-1/2}^{n-1/2} - \frac{\Delta t}{\mu} \left( \frac{E_y \Big|_{i+3/2, j-1/2}^n - E_y \Big|_{i+1/2, j-1/2}^n}{\Delta z} \right) \\ E_y \Big|_{i, j+1/2}^{n+1} = E_y \Big|_{i, j+1/2}^n + \frac{\Delta t}{\varepsilon} \left( \frac{H_x \Big|_{i, j+1}^{n+1/2} - H_x \Big|_{i, j}^{n+1/2}}{\Delta z} \right) - \frac{\Delta t}{\varepsilon} \left( \frac{H_z \Big|_{i+1/2, j+1/2}^{n+1/2} - H_z \Big|_{i-1/2, j+1/2}^{n+1/2}}{\Delta x} \right) \end{array} \right.$$

# Numerical dispersion

- Numerical dispersion means dependence of phase velocity on wavelength, direction of propagation and lattice discretisation.
- It can lead to pulse distortion, artificial anisotropy and pseudo-refraction.

$$\left[ \frac{1}{\Delta x} \sin\left(\frac{k_x \Delta x}{2}\right) \right]^2 + \left[ \frac{1}{\Delta z} \sin\left(\frac{k_z \Delta z}{2}\right) \right]^2 = \left[ \frac{1}{c \cdot \Delta t} \sin\left(\frac{\omega \Delta t}{2}\right) \right]^2$$



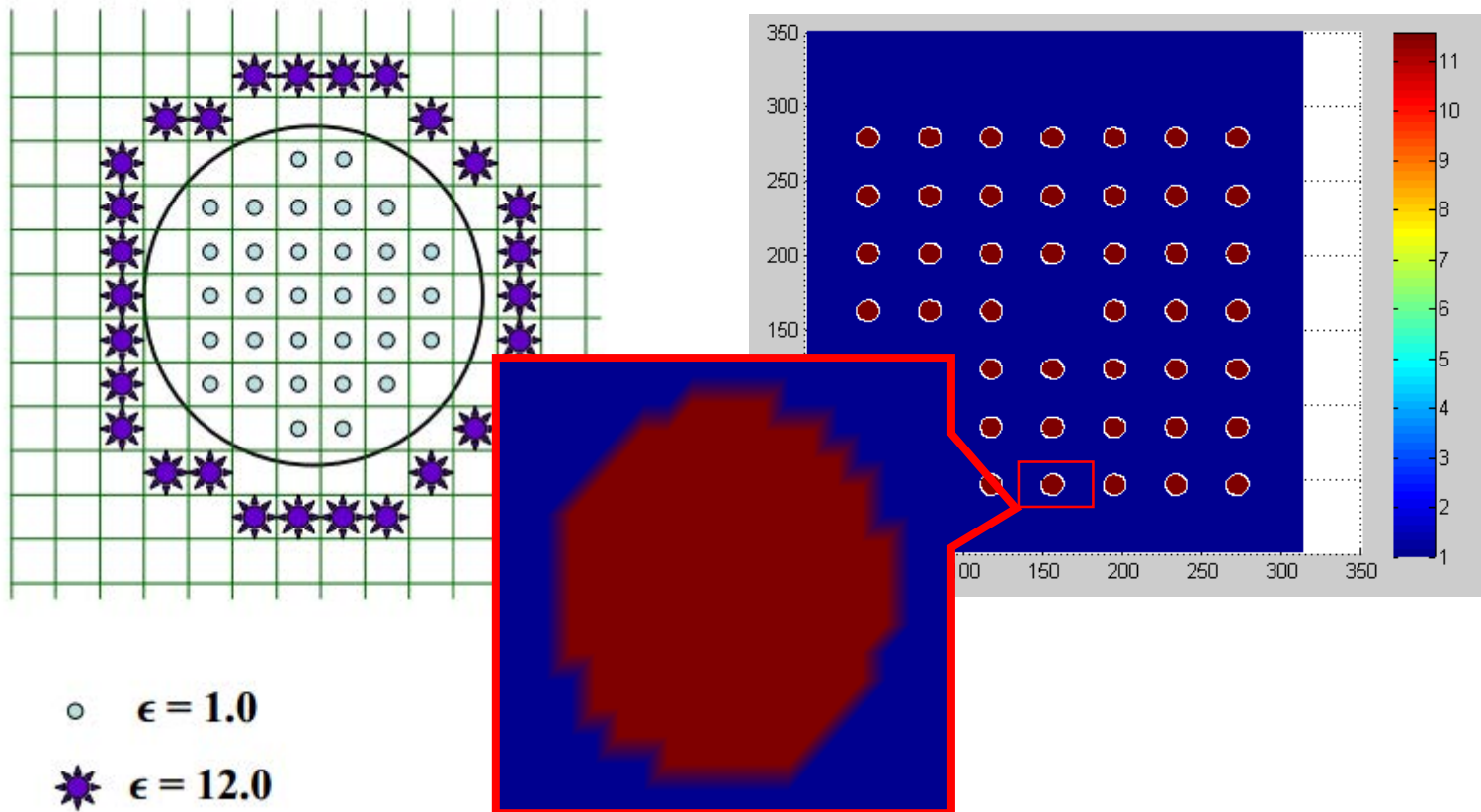
- The numerical stability of the method is ensured by **Courant-Friedrichs-Levy (CFL) condition**

$$\Delta t \leq \frac{1}{c \sqrt{\frac{1}{(\Delta x)^2} + \frac{1}{(\Delta z)^2}}}$$

- $c$  is the light velocity
- $\Delta x$  is the discretisation along  $x$  direction
- $\Delta z$  is the discretisation along  $z$  direction

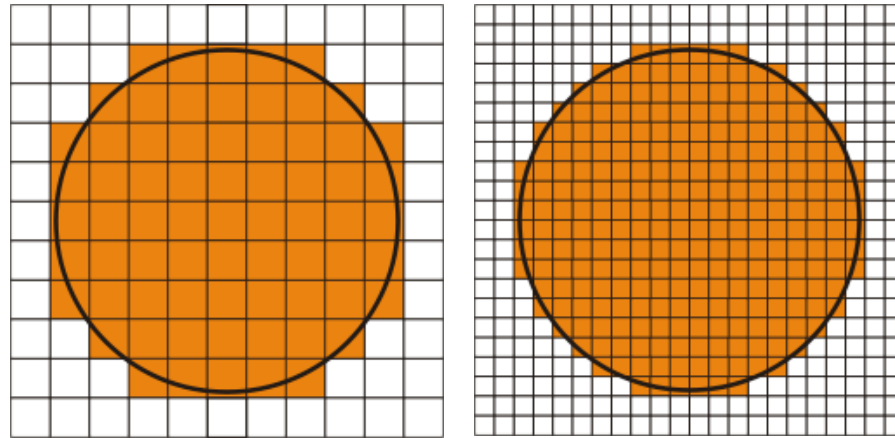
## Meshing and staircase problem

**Grids:** collocated or staggered, rectangular or hexagonal, orthogonal, non-orthogonal or curvilinear, structured or unstructured, regular or irregular

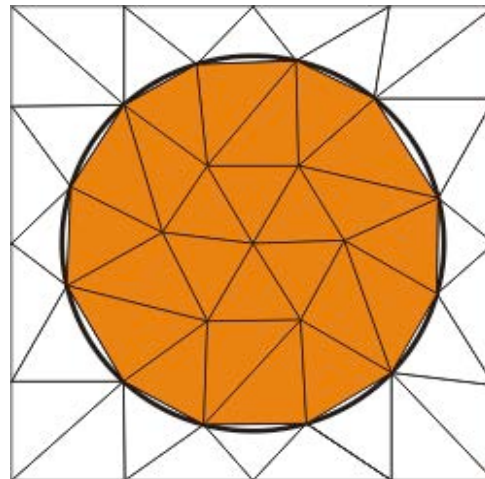


# Meshing and staircase problem

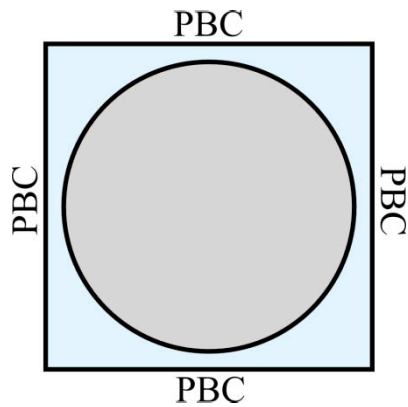
## structured mesh



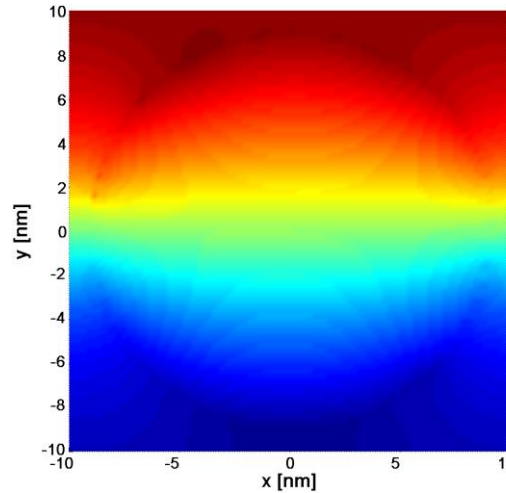
## unstructured mesh



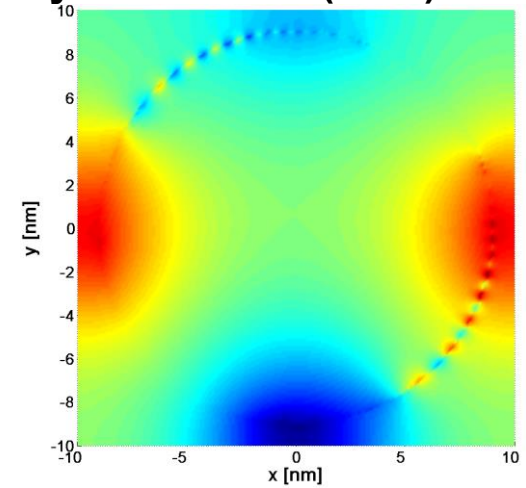
# Silver nanorod modes: the unit cell



## FDTD – Periodic Boundary Conditions (PBC)

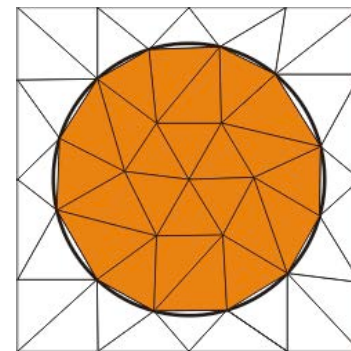
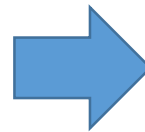
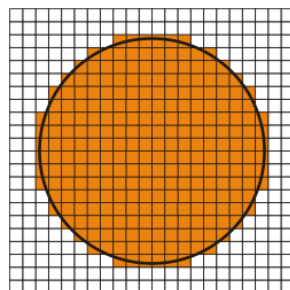
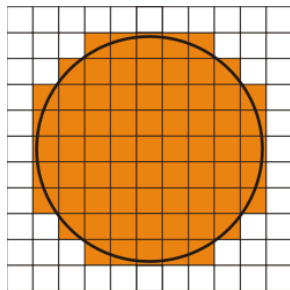


$\lambda = 438.9 \text{ nm}$



$\lambda = 235.8 \text{ nm}$

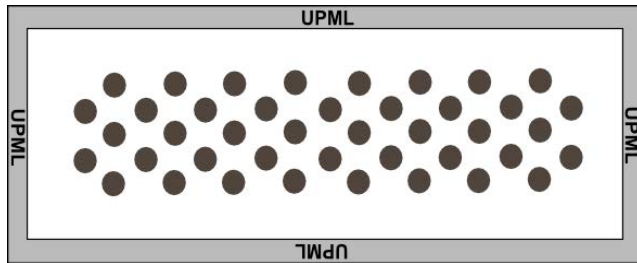
## A possible solution: FVTD - PBC





# Silver nanorods waveguide

## 2D plasmonic waveguide on Silver nanorods in hexagonal lattice



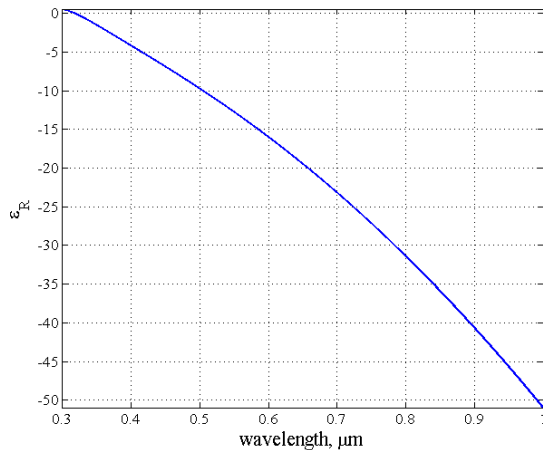
$$a = 200 \text{ nm}$$

$$r = 0.25 a$$

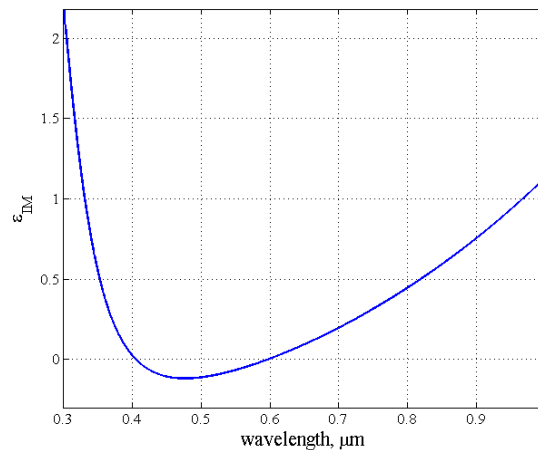
$$\lambda = 600 \text{ nm}$$



Real part of  $\epsilon$



Imaginary part of  $\epsilon$

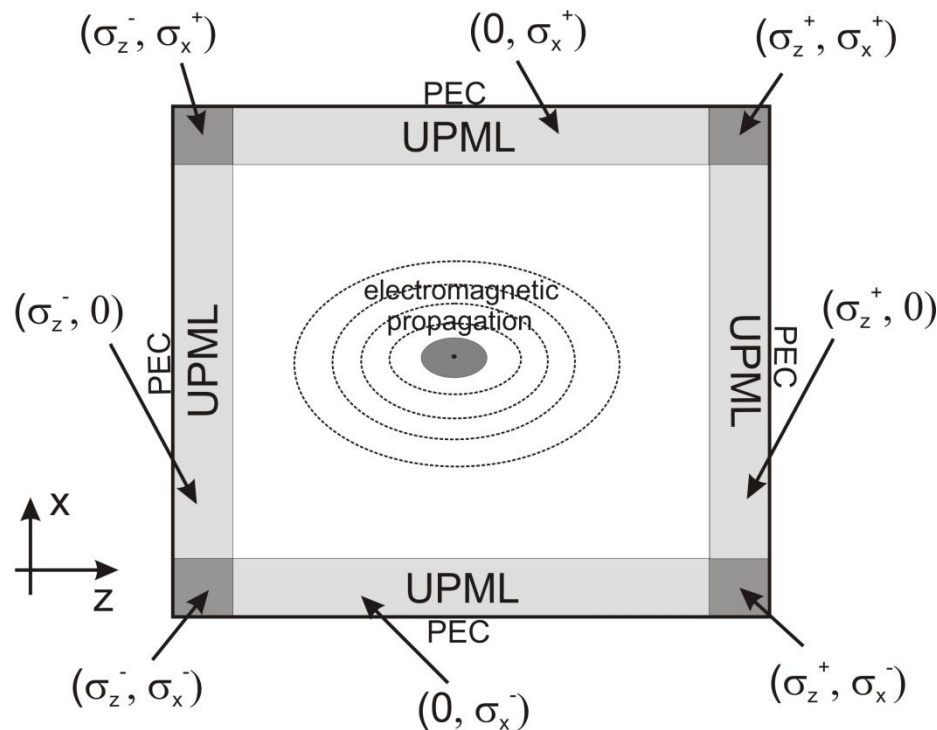


The Silver complex dielectric constant is modelled by **Drude–Critical Points** model and solved into Auxiliary Differential Equation (**ADE**) scheme

# Truncation of the computational window

- Periodic Boundary Conditions (PBC)
- Absorbing Boundary Conditions (ABC)
  - analytical (Mur's ABC)
  - perfectly matched layers (PML)
- PEC, PMC

## Uniaxial Perfectly Matched Layers (UPML)



# Uniaxial Perfectly Matched Layers (UPML)

Gedney, 1996

$$\nabla \times \bar{E} = -j\omega\mu_0 \bar{\mu} \bar{H}$$

$$\nabla \times \bar{H} = j\omega\varepsilon_0 \bar{\varepsilon} \bar{E}$$

$$\bar{\varepsilon} = \bar{\mu} = \begin{bmatrix} \frac{s_y s_z}{s_x} & 0 & 0 \\ 0 & \frac{s_x s_z}{s_y} & 0 \\ 0 & 0 & \frac{s_x s_y}{s_z} \end{bmatrix}$$

$$B_x \Big|_{i,j+\frac{1}{2}}^{n+\frac{1}{2}} = B_x \Big|_{i,j+\frac{1}{2}}^{n-\frac{1}{2}} + \frac{\Delta t}{\Delta z_j} \left( E_y \Big|_{i,j+1}^n - E_y \Big|_{i,j}^n \right)$$

$$s_i = k_i + \frac{\sigma_i}{j\omega\varepsilon_0} \quad (i = x, y, z)$$

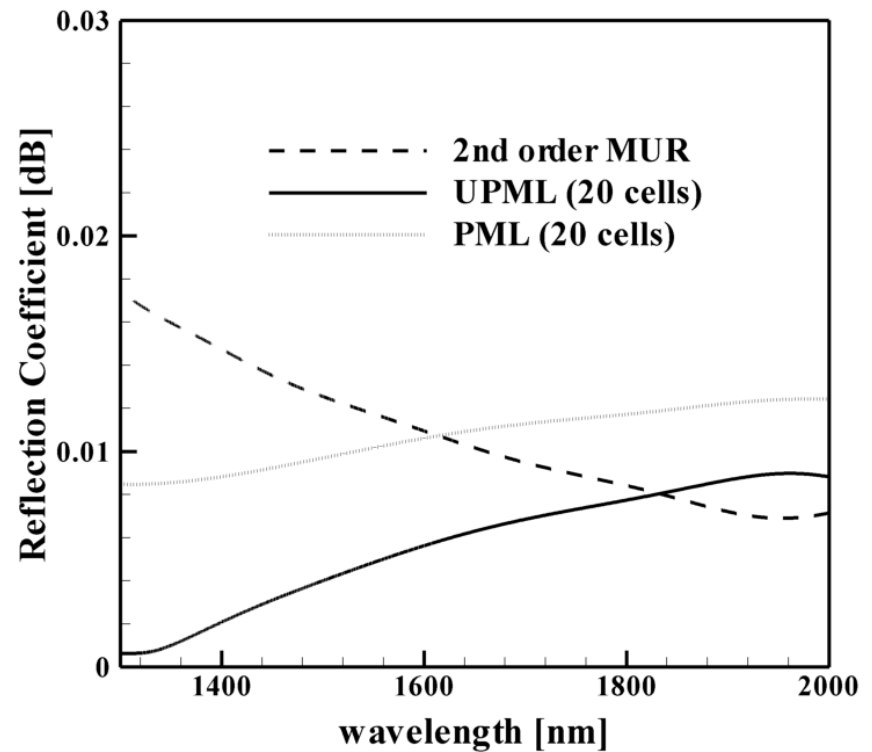
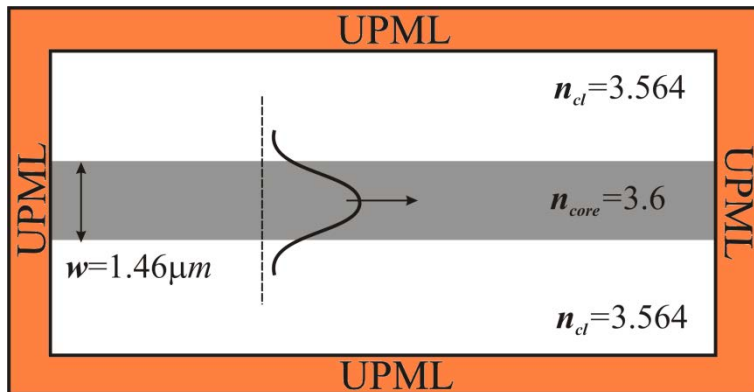
$$H_x \Big|_{i,j+\frac{1}{2}}^{n+\frac{1}{2}} = \left( \frac{2\varepsilon_0 - \sigma_z \Delta t}{2\varepsilon_0 + \sigma_z \Delta t} \right) H_x \Big|_{i,j+\frac{1}{2}}^{n-\frac{1}{2}} + \left( \frac{2\varepsilon_0 + \sigma_x \Delta t}{2\varepsilon_0 + \sigma_z \Delta t} \right) \frac{1}{\mu_0} B_x \Big|_{i,j+\frac{1}{2}}^{n+\frac{1}{2}} - \left( \frac{2\varepsilon_0 - \sigma_x \Delta t}{2\varepsilon_0 + \sigma_z \Delta t} \right) \frac{1}{\mu_0} B_x \Big|_{i,j+\frac{1}{2}}^{n-\frac{1}{2}}$$

$$D_y \Big|_{i,j}^{n+1} = \left( \frac{2\varepsilon_0 - \sigma_z \Delta t}{2\varepsilon_0 + \sigma_z \Delta t} \right) D_y \Big|_{i,j}^n + \frac{1}{h_z^j} \left( \frac{2\varepsilon_0 \Delta t}{2\varepsilon_0 + \sigma_z \Delta t} \right) \left( H_x \Big|_{i,j+\frac{1}{2}}^{n+\frac{1}{2}} - H_x \Big|_{i,j-\frac{1}{2}}^{n+\frac{1}{2}} \right) - \frac{1}{h_x^i} \left( \frac{2\varepsilon_0 \Delta t}{2\varepsilon_0 + \sigma_z \Delta t} \right) \left( H_z \Big|_{1+\frac{1}{2},j}^{n+\frac{1}{2}} - H_z \Big|_{1-\frac{1}{2},j}^{n+\frac{1}{2}} \right)$$

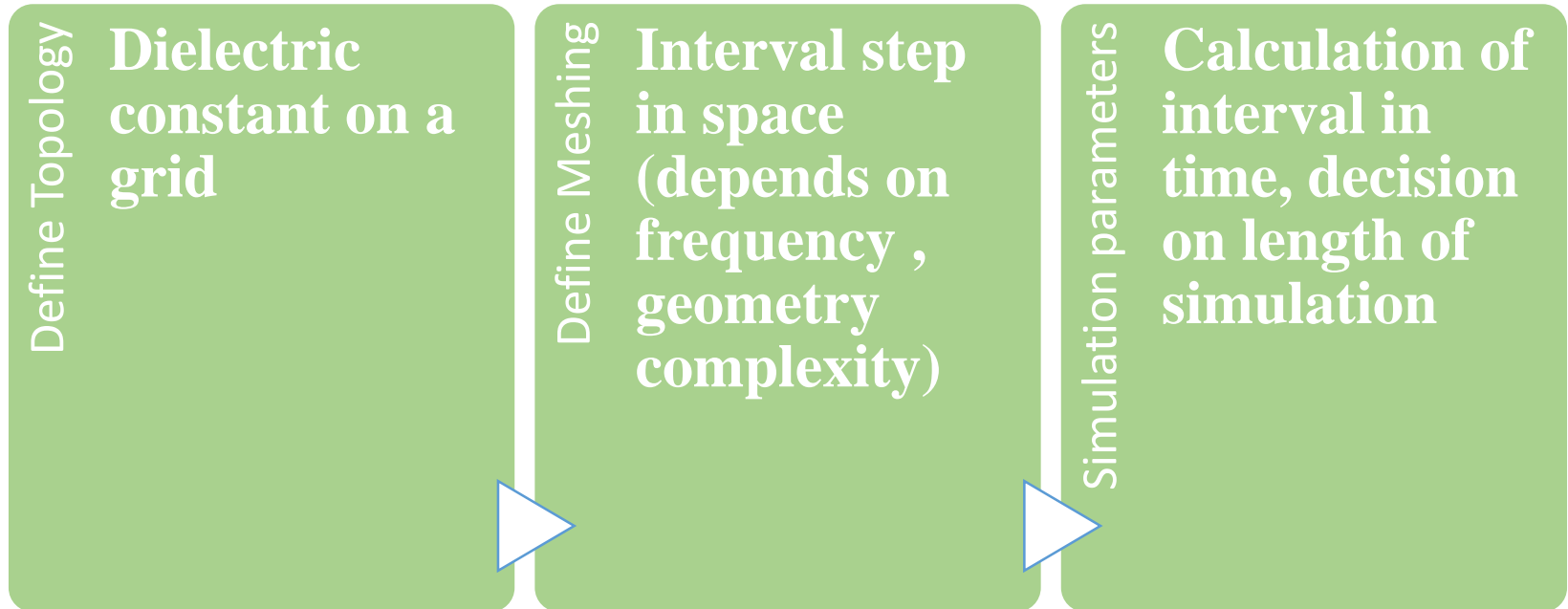
$$E_y \Big|_{i,j}^{n+1} = \left( \frac{2\varepsilon_0 - \sigma_x \Delta t}{2\varepsilon_0 + \sigma_x \Delta t} \right) E_y \Big|_{i,j}^n + \left( \frac{2\varepsilon_0}{2\varepsilon_0 + \sigma_x \Delta t} \right) \frac{1}{\varepsilon} \left( D_y \Big|_{i,j}^{n+1} - D_y \Big|_{i,j}^n \right)$$

# Truncation of the computational window

## Comparison of different boundary schemes to truncate an optical waveguide



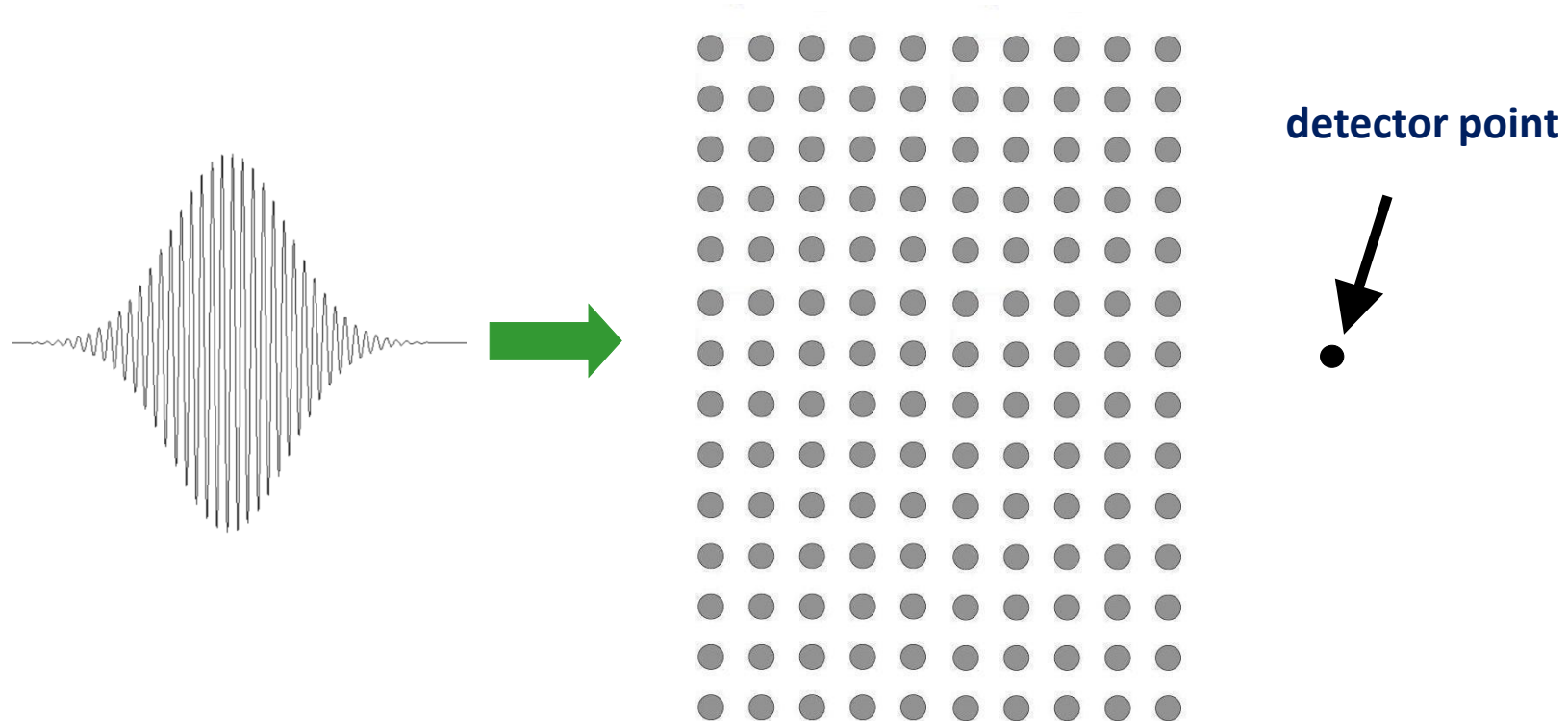
# Implementation



# Determination of the photonic bandgap

A wide broadband plane wave pulse is sent towards the photonic crystal

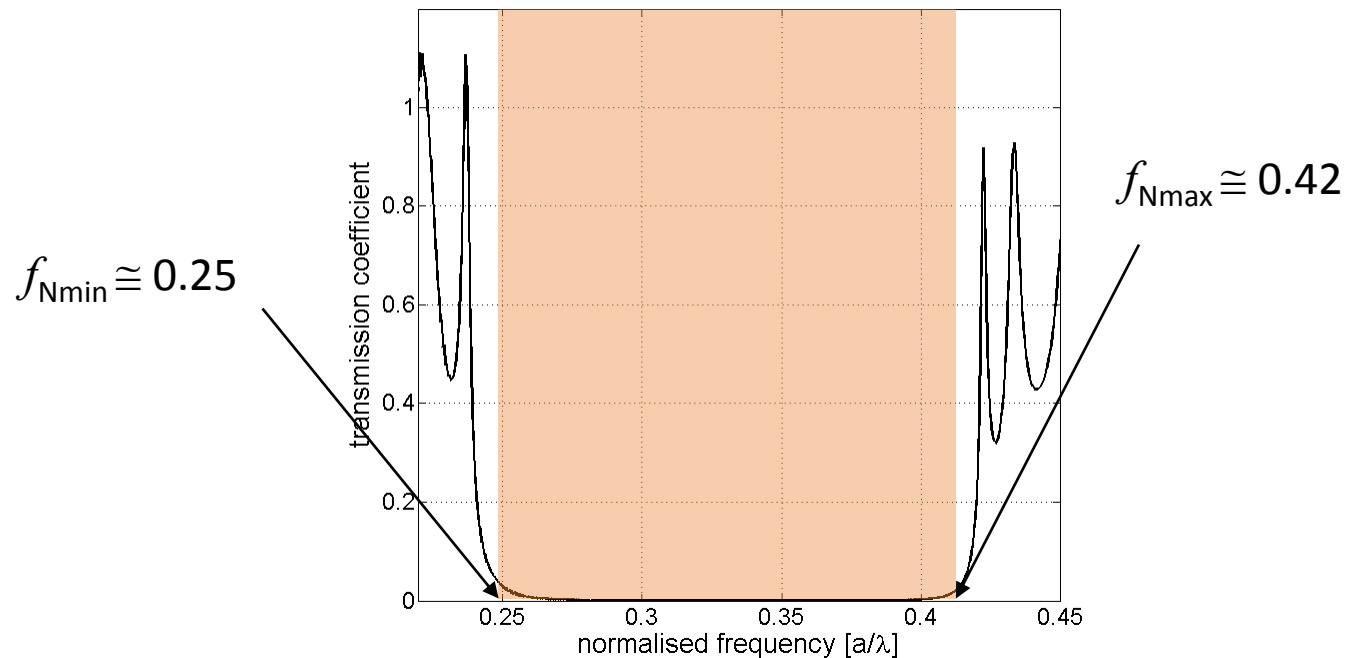
The time-domain variations of the incident and transmitted fields are stored for all time steps of the simulation at some detectors



# Determination of the photonic bandgap

The FFT of the stored incident and transmitted fields is performed and the transmission coefficient is calculated

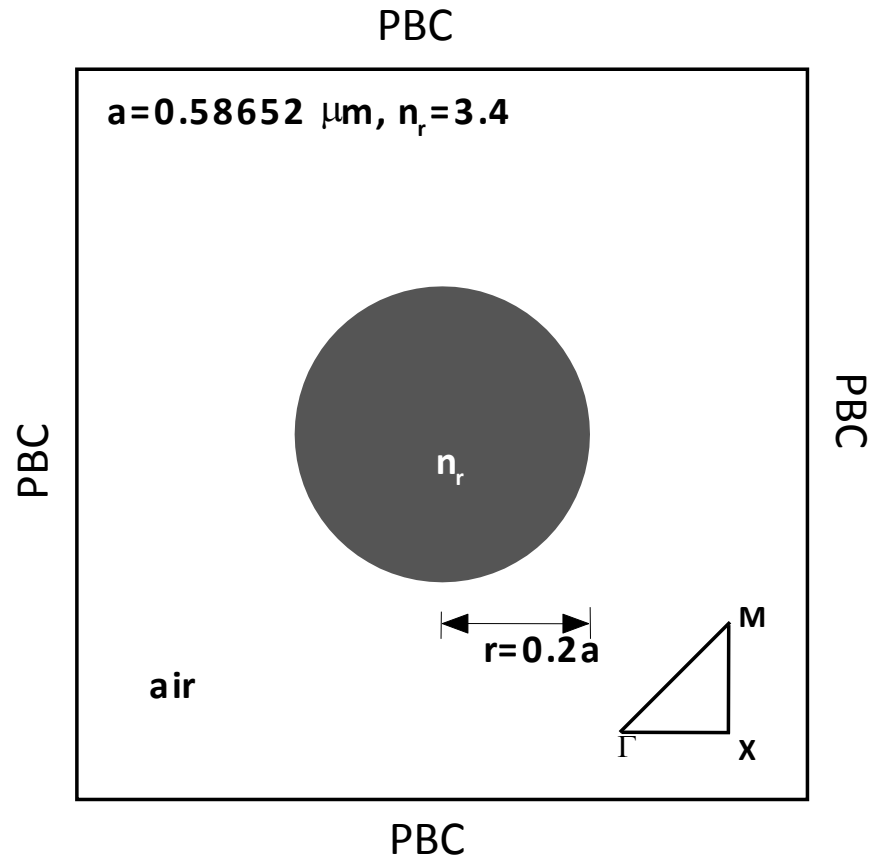
The photonic bandgap (PBG) is determined by the range of normalised frequencies for which the transmission is zero.



$$\text{PBG} = f_{N\text{max}} - f_{N\text{min}} \cong [0.42 - 0.25] = 0.17$$

# Determination of the photonic bandgap

Another method to determine the photonic band gap for a fixed photonic crystal lattice is to consider the unit cell of the crystal itself and applying the periodic boundary conditions (PBCs)





## Determination of the photonic bandgap

To apply periodic boundary conditions, the electric and magnetic fields are splitted into sine and cosine components as:

$$\bar{e}_1(\bar{r} + \bar{R}; t) = \bar{e}_1(\bar{r}; t) \cos(\bar{k} \cdot \bar{R}) - \bar{e}_2(\bar{r}; t) \sin(\bar{k} \cdot \bar{R})$$

$$\bar{e}_2(\bar{r} + \bar{R}; t) = \bar{e}_1(\bar{r}; t) \sin(\bar{k} \cdot \bar{R}) + \bar{e}_2(\bar{r}; t) \cos(\bar{k} \cdot \bar{R})$$

$$\bar{e}_1(\bar{r}; t) = \bar{e}_1(\bar{r} + \bar{R}; t) \cos(\bar{k} \cdot \bar{R}) + \bar{e}_2(\bar{r} + \bar{R}; t) \sin(\bar{k} \cdot \bar{R})$$

$$\bar{e}_2(\bar{r}; t) = -\bar{e}_1(\bar{r} + \bar{R}; t) \sin(\bar{k} \cdot \bar{R}) + \bar{e}_2(\bar{r} + \bar{R}; t) \cos(\bar{k} \cdot \bar{R})$$

where the subscripts *1* and *2* denote the sine and cosine components, respectively, *R* stands for the lattice constant vector, and *k* stands for the wavevector. The above equations, together with the analogous for the magnetic fields, are inserted in the FDTD scheme to update the field components at periodic boundaries.

# Determination of the photonic bandgap

- The excitation source takes the form of a current source whose expression is given as

$$J_s = \sin(2\pi f_0 t) e^{-\left(\frac{2(t-t_0)}{T_0}\right)^2} e^{-\left(\frac{2(y-y_0)}{W_0}\right)^2} e^{-\left(\frac{2(z-z_0)}{W_0}\right)^2}$$

- where  $f_0$  is the modulation frequency,  $t_0$  is the time delay,  $T_0$  is the time-width, and  $y_0$ ,  $z_0$ , are the centre of the source, and  $W_0$  is the space-width of the pulse.
- The wavevector  $k$  is set according to the irreducible Brillouin zone.
- The time-variation of the electric field is recorded at different observation points until steady-state is reached.
- Upon using FFT, the spectrum of the time-domain response is obtained.
- This spectrum presents peaks that correspond to all the eigenmodes compatible with periodic boundary applied to terminate the unit cell.

# Determination of the photonic bandgap

$a = 0.58652 \mu\text{m}, n_r = 3.4$   
 $a = 0.2a$

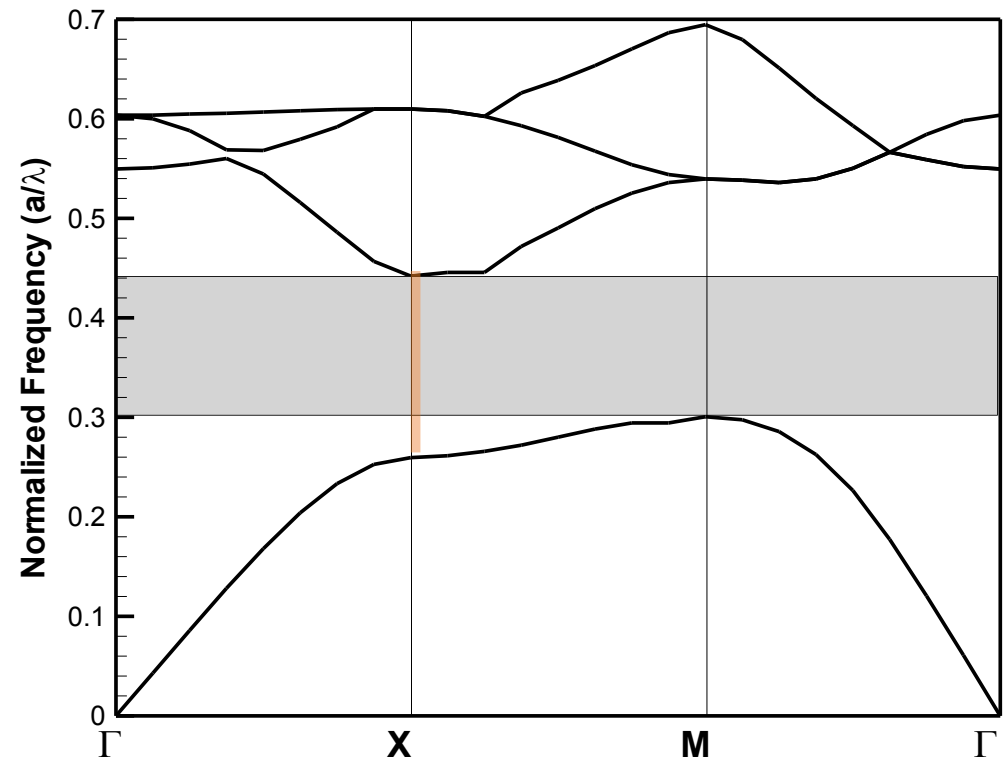
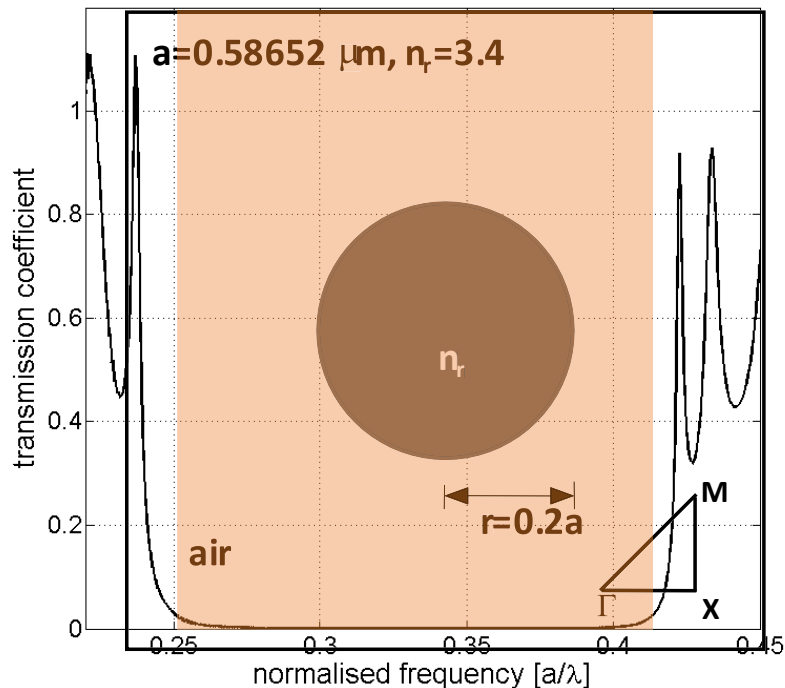
$\vec{e}_1(\vec{r} + \vec{R}; t) = \vec{e}_1(\vec{r}; t) \cos(\vec{k} \cdot \vec{R}) - \vec{e}_2(\vec{r}; t) \sin(\vec{k} \cdot \vec{R})$   
 $\vec{e}_2(\vec{r} + \vec{R}; t) = \vec{e}_1(\vec{r}; t) \sin(\vec{k} \cdot \vec{R}) + \vec{e}_2(\vec{r}; t) \cos(\vec{k} \cdot \vec{R})$

$\vec{e}_1(\vec{r}; t) = \vec{e}_1(\vec{r} + \vec{R}; t) \cos(\vec{k} \cdot \vec{R}) + \vec{e}_2(\vec{r} + \vec{R}; t) \sin(\vec{k} \cdot \vec{R})$   
 $\vec{e}_2(\vec{r}; t) = -\vec{e}_1(\vec{r} + \vec{R}; t) \sin(\vec{k} \cdot \vec{R}) + \vec{e}_2(\vec{r} + \vec{R}; t) \cos(\vec{k} \cdot \vec{R})$

The phase shift is changed according to the wavevector  $k$  varied along the irreducible Brillouin zone.

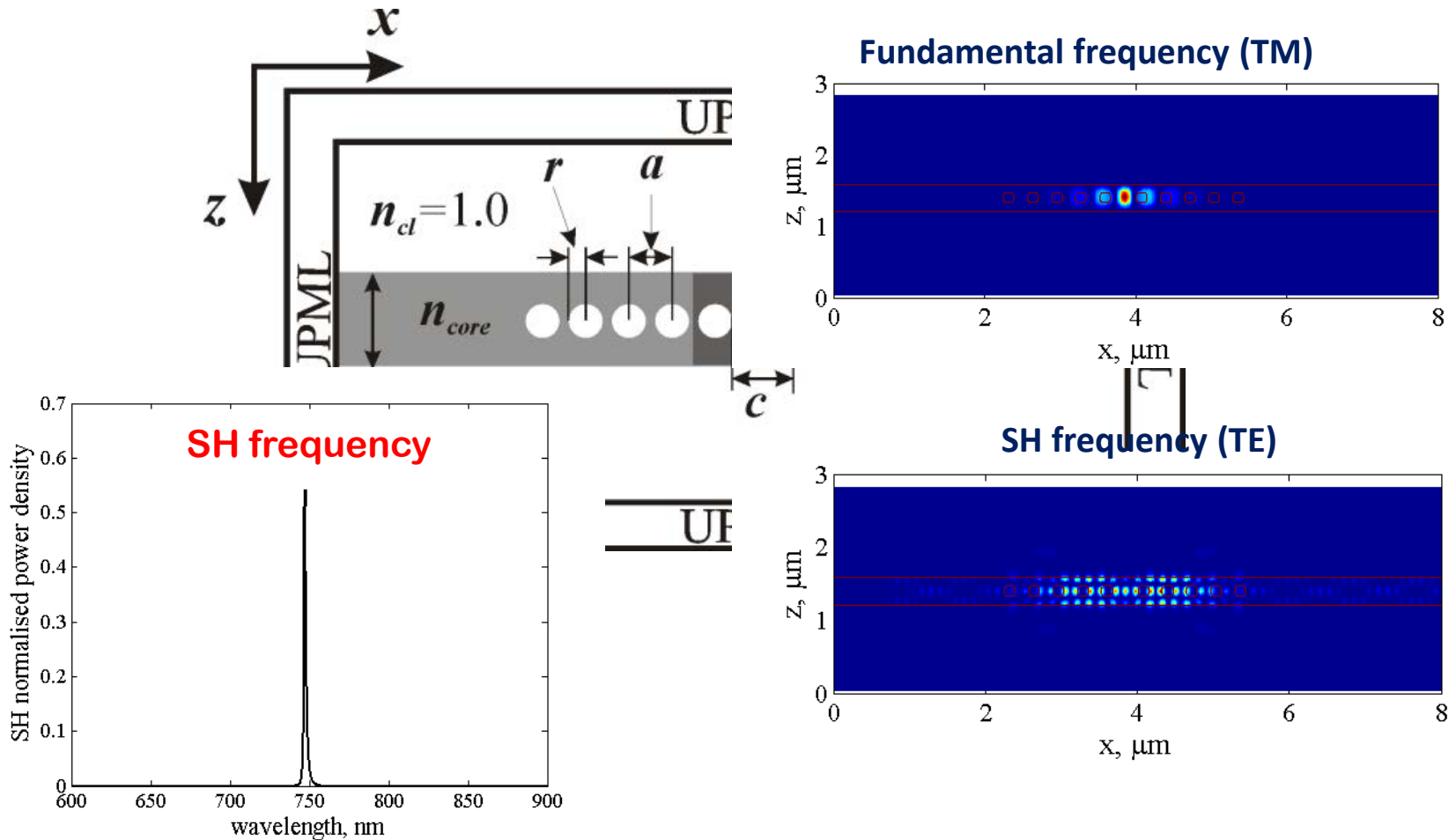
# Determination of the photonic bandgap

Varying  $k$  along the Brillouin zone and extracting all the eigenmodes for each value of  $k$ , it is possible to extract the photonic bandgap associated with the photonic crystal.



# Nonlinear FDTD

## Enhanced Second Harmonic Generation



## FDTD codes

- MEEP/MPB solvers:
  - [http://ab-initio.mit.edu/wiki/index.php/Meep\\_Introduction](http://ab-initio.mit.edu/wiki/index.php/Meep_Introduction)
- FDTD++ (JFDTD):
  - <https://www.fdtddxx.com/about>
- A number of other 1D and 2D FDTD codes are available online, mainly in Matlab.

# Conclusions

- Both metamaterials and plasmonics provide new electromagnetic properties which can modify the interaction with particle beams.
  - Metamaterials explored in the microwave range.
  - Plasmonics can offer an alternative to dielectric photonic structures for high frequency acceleration.
- Choice of materials/geometry of inclusions is crucial.
- Limitations need to be clearly identified.